

## Effect of electrostatic interaction on the retention and remobilization of colloidal particles in porous media

Kottsova, Anna K.; Mirzaie Yegane, Mohsen; Tchistiakov, Alexei A.; Zitha, Pacelli L.J.

**DOI**

[10.1016/j.colsurfa.2021.126371](https://doi.org/10.1016/j.colsurfa.2021.126371)

**Publication date**

2021

**Document Version**

Accepted author manuscript

**Published in**

Colloids and Surfaces A: Physicochemical and Engineering Aspects

**Citation (APA)**

Kottsova, A. K., Mirzaie Yegane, M., Tchistiakov, A. A., & Zitha, P. L. J. (2021). Effect of electrostatic interaction on the retention and remobilization of colloidal particles in porous media. *Colloids and Surfaces A: Physicochemical and Engineering Aspects*, 617, 1-12. Article 126371. <https://doi.org/10.1016/j.colsurfa.2021.126371>

**Important note**

To cite this publication, please use the final published version (if applicable). Please check the document version above.

**Copyright**

Other than for strictly personal use, it is not permitted to download, forward or distribute the text or part of it, without the consent of the author(s) and/or copyright holder(s), unless the work is under an open content license such as Creative Commons.

**Takedown policy**

Please contact us and provide details if you believe this document breaches copyrights. We will remove access to the work immediately and investigate your claim.

# Colloids and Surfaces A: Physicochemical and Engineering Aspects

## Effect of electrostatic interaction on the retention and remobilization of colloidal particles in porous media

--Manuscript Draft--

|                              |   |
|------------------------------|---|
| <b>Manuscript Number:</b>    | COLSUA-D-20-03864R1   |
| <b>Article Type:</b>         | Research Paper  |
| <b>Keywords:</b>             | colloidal fines; hematite particles; point of zero charge; van der Waals; electrostatic interactions  |
| <b>Corresponding Author:</b> | Anna Kottsova<br><br>RUSSIAN FEDERATION   |
| <b>First Author:</b>         | Anna K. Kottsova  |
| <b>Order of Authors:</b>     | Anna K. Kottsova<br>Mohsen Mirzaie Yegane<br>Alexei A. Tchistiakov<br>Pacelli L.J. Zitha  |
| <b>Abstract:</b>             | We investigate the effect of pH on external hematite colloidal particles entrapment and remobilization by core-flood experiments combined with X ray computed tomography. Suspensions of calibrated hematite colloidal particles were injected into Bentheimer sandstones sample, composed mainly of well-sorted quartz and small clay fraction (up to 1 wt%), consisting mainly of kaolinite. We have found that permeability impairment due to an external cake build-up can be reversed when pH exceeds the point of zero charge of hematite particles. This effect could be successfully interpreted by the switching of the surface charge of hematite particles from positive to the negative, similar to the rock surface. The experimentally verified pH-controlled electrostatic retention and remobilization technique can be extended to other colloidal particles, having pH-dependent surface charge, including natural clay minerals in hydrocarbon and geothermal reservoirs. Therefore, varying pH of injected fluid can be applied for targeted external cake build-up and transportation of colloidal particles within a reservoir. |



Skolkovo Institute of Science and Technology

Anna Kottsova

PhD student

Skolkovo Institute of Science and Technology

Center for Hydrocarbon Recovery

Dear Sir / Madam,

We submit for your consideration the revised manuscript COLSUA-D-20-03864 entitled “Effect of electrostatic interaction on the retention and remobilization of colloidal particles in porous media” by Anna K. Kottsova, Mohsen Mirzaie Yegane, Alexei A. Tchistiakov and Pacelli L.J. Zitha. We carefully considered valuable comments of the reviewers on the initial manuscript and made corresponding revisions in the text.

In this research we investigated the impact of electrostatic interaction, controlled by pH alteration, on entrapment and remobilization of hematite colloidal particles in a sandstone porous medium. It was experimentally found that permeability reduction due to external cake build-up can be reversed and the particles captured near the inlet core surface can be remobilized, when pH exceeds the point of zero charge and the sign of the particles surface charge becomes similar to the one of quartz grains. The research establishes that for colloidal particles the electrostatic retention mechanism can dominate over the size-exclusion mechanism, which traditionally serves as an explanation of permeability impairment, caused by external fines during water flooding. Therefore, varying pH of injected fluid can be applied for targeted external cake build-up control and transportation of colloidal particles within a reservoir. The results of this study provide insights into fine-tuning the electrostatic interactions in porous media and thus mitigating the permeability reduction as a result of fines migration. The experimentally verified technique can be extended to other particles with pH-dependent surface charge, including natural minerals in hydrocarbon and geothermal reservoirs.

Thank you very much for your consideration of our article. We look forward to hearing from you.

Sincerely,

A handwritten signature in black ink, appearing to read "Anna Kottsova".

Anna Kottsova

We thank the reviewers for their careful assessment of our paper COLSUA-D-20-03864 titled “Effect of electrostatic interaction on the retention and remobilization of colloidal particles in porous media”. We have carefully considered the recommendations and made corresponding revisions in the text that are summarized in the comments below.

**Reviewer #1:**

*Deposition and detachment of hematite in sandstone are discussed in this manuscript. The authors show that re-migration of deposited hematite is possible by increasing pH due to the development of electric double layer repulsion. While the manuscript seems to have useful information, revision is necessary by addressing the following points.*

**Reviewer Point P1.1.** *I strongly suggest the authors to add successive line numbers in all the manuscripts.*

**Reply P1.1.** The recommendation is applied in the revised manuscript.

**Reviewer Point P1.2.** *page 2, line 4. This paragraph has one sentence. The paragraph structure should be reconsidered.*

**Reply P1.2.** The corresponding correction has been made in the text (page 2).

**Reviewer Point P1.3.a** *page 2, middle part. The authors summarize the effect of electric double layer (EDL) attraction between colloidal particles and surface of materials composing porous media on the deposition. With attractive EDL force, the deposition does not strongly depend on the magnitude of surface potential controlled by pH (e.g. <https://doi.org/10.1016/j.colsurfa.2008.09.054> ).*

**Reply P1.3.a** The introduction was reviewed accordingly (page 3, lines 1-5):

‘Kumar et al. (2017) has experimentally shown that an increase of pH causes increase of the magnitude of the long-range repulsion between a SiO<sub>2</sub> tip and a silica facet of kaolinite. The experiments were done within the range of pH above kaolinite’s PZL and thus no charge reversal occurred. Kobayashi et al. (2009) have investigated the effect of pH alteration on retention of latex particles by a zirconia bed and concluded that pH increase had minor effect on the retention in comparison with salinity rise.’

**Reviewer Point P1.3.b**

*But, in the later stage of deposition, deposition behavior depend the lateral interaction between deposited particles (e.g. [https://www.jstage.jst.go.jp/article/jscejam/70/2/70\\_1\\_743/article/-char/ja/](https://www.jstage.jst.go.jp/article/jscejam/70/2/70_1_743/article/-char/ja/)). These points are not discussed.*

**Reply P1.3.** This phenomenon is considered in the Results and Discussion section 3.3 (page 12, lines 22-25):

‘The formation of the external filter cake could occur due to electrostatic retention of positively charged hematite particles by negatively charged quartz matrix. Although at later stages of deposition, when quartz surfaces got considerably covered by hematite particles, they could produce lateral repulsion effects (Kobayashi et al., 2014) screening the electrostatic attraction of quartz surfaces.’

**Reviewer Point P1.4.** *In the later part of Introduction, the authors describe what they have done. The purpose and question of this research are unclear to me. Also, the authors should emphasize the novelty and significance of their finding.*

**Reply P1.4.** The Introduction was reviewed accordingly to highlight the purpose (objective) of our research (page 3, lines 9-13):

‘The main objective of this research was to examine the possibility of artificial management of external colloidal particles retention by natural sandstone matrix and remobilization by gradual increase of pH of the injected fluid above the mineral point of zero charge. In previous studies pressure and effluent data were mainly used for monitoring fines migration within rock porous media, in the present study next to differential pressure measurements we applied X-ray tomography for tracking the migration of remobilized particles.’

The novelty of the results was also emphasized in the General Discussion section (page 15, lines 21-28):

‘Generally, our work is in agreement with the aforementioned studies on the hypothesis of mobilization of particles with a pH-dependent surface charge at a high pH level. As the step forward in the ongoing research we provide a detailed theoretical study of colloidal stability of hematite particles and report the effect of surface charge density of particles and rock matrix on the electrostatic interaction between them. Moreover, we experimentally established the theoretical possibility of external particles remobilization and migration because of their charge reversal caused by

pH increase, by means of variety of methods, including CT scanning technique that proved to be an effective tool for monitoring the migration of colloidal particles in the porous media throughout the experiment.<sup>7</sup>

**Reviewer Point P1.5.** Does "demi-water" mean deionized water? Using "demi-water" is very rare, I guess.

**Reply P1.5.** The proposed change was accepted and implemented in the text.

**Reviewer Point P1.6.** Eq. (4). "x" should be in italic, and "ln" should not be in italic.

**Reply P1.6.** The suggested changes were implemented in the text.

**Reviewer Point P1.7.** The authors should explain Eq. (7). What is the distance to the shear plane, where zeta potential is defined, from the particle surface?

**Reply P1.7.** In Eq. (7), we estimate the surface potential from zeta potential by solving the Poisson–Boltzmann equation for a distribution of the point charges that decay as a function of the radial distance from the charged particle surface<sup>1</sup> (zeta-potential is the value of the electrostatic potential on the imaginary slipping plane, also termed the surface of hydrodynamic shear, that is the surface where particles interact with one another or with other surfaces<sup>2</sup>). In this equation, it is assumed that the local dielectric constant around a particle is independent of the radial distance from the surface, and that the energy required to transport charges in solution depends only on Coulomb interactions.<sup>3</sup> This approach has been discussed in literature<sup>1, 3, 4</sup> (see below).

To provide more clarity, the following has been added to the revised manuscript (*page 7, lines 7-9*):

*'Equation 7 is obtained by solving the Poisson–Boltzmann equation for a distribution of the point charges that decay as a function of the radial distance from the surface of charged particle.'*<sup>1</sup>

#### References

1. Wijenayaka, L. A.; Ivanov, M. R.; Cheatum, C. M.; Haes, A. J., Improved Parametrization for Extended Derjaguin, Landau, Verwey, and Overbeek Predictions of Functionalized Gold Nanosphere Stability. *The Journal of Physical Chemistry C* 2015, 119, (18), 10064-10075.
2. Lowry, G. V.; Hill, R. J.; Harper, S.; Rawle, A. F.; Hendren, C. O.; Klaessig, F.; Nobbmann, U.; Sayre, P.; Rumble, J., Guidance to improve the scientific value of zeta-potential measurements in nanoEHS. *Environmental Science: Nano* 2016, 3, (5), 953-965.
3. Sonntag, H., Strenge, K., *Coagulation Kinetics and Structure Formation*. Springer US: New York, 1987.
4. Ohshima, H., *Effective Surface Potential and Double-Layer Interaction of Colloidal Particles*. *Journal of Colloid and Interface Science* 1995, 174, (1), 45-52.

**Reviewer Point P1.8.** Eqs. (9) and (10), SOH should be SiOH, because the authors assume the sandstone is more or less silica like.

**Reply P1.8.** This equation is based on the surface charge of siliceous minerals (S represents the minerals) due to the ionization reactions of the surface OH groups. We agree with the reviewer, that we can change it to Si to make it specific for Silica. The suggested changes were implemented in the text (*page 9, eq. (10), (11)*).

**Reviewer Point P1.9.** What kind of theoretical equations are used when calculating zeta potential?

**Reply P1.9.** The corresponding information is added to the section 2.4.3. (*page 6, line 12*).

**Reviewer Point P1.10.** What about the effect of electrolyte concentration on the charge density and zeta potential? The charge density and zeta potential (electrophoretic mobility) of silica and hematite vary with pH and salt concentration (e.g. <https://doi.org/10.1006/jcis.1997.5207> and <https://doi.org/10.1021/la046829z>). Do the authors consider the effect of salt concentration on charging when drawing the potential curves with DLVO theory? What are zeta potential at each salt concentration and pH used in the calculation with DLVO theory?

**Reply P1.10.** Indeed, we did consider the effect of salt concentration on zeta potential while calculating the potential curves with DLVO theory. The effect of ionic strength on hematite particle interaction at pH 5.8 was shown in Figure

7a. The impact of increasing electrolyte concentration was reflected in decreasing Debye length (according to Equation 6), which results in decreasing the inter-particle interaction potential ( $V_i$ ).

Following the reviewer's comment, we performed additional experiments to measure zeta potential at various ionic strength at pH 5.8. Figure 7a has been modified accordingly. However, this has not changed the conclusion of this study (page 11, lines 3-5):

*'Nonetheless, increasing the ionic strength to 50, 85 and 200 mM led to a potential barrier smaller than 15/kBT implying that the colloidal stability is not achieved.'*

Concerning the second question regarding *zeta potential values at each salt concentration and pH used in the calculation with DLVO theory* we would like to mention that Figure 6 shows zeta potential at various pH at  $I=1$  mM. In order to address the comment of the reviewer we have also added a table with corresponding zeta potential values in the supplementary materials (Table S2, page 2-3).

**Reviewer Point P1.11.** page 14-. *General discussion.*

*Here, the authors discuss aggregate/floc breakup as "deflocculation" of aggregates. I agree with the importance of aggregate breakup during transport. Breakup of aggregate/floc is also controlled by hydrodynamic condition and aggregate strength (e.g. <https://doi.org/10.1016/j.watres.2005.05.037>). Did the change in flow condition affect transport and remigration of particle in this study?*

**Reply P1.11.** The reviewer raised a valid point and we agree that hydrodynamic force can have an impact on colloidal particle transportation. This is acknowledged in the Introduction. However, in this research we concentrated on the study of pH effect only and thus maintained the same flow rate for all pH values during the experiments.

**Reviewer Point P1.12.** *The authors also emphasize the importance of charge reversal by changing pH. Hematite undergoes charge reversal in the presence of anionic surfactants (e.g. <https://doi.org/10.1016/j.colsurfa.2016.07.063>). It might be easier by adding surfactants instead of varying pH. So, it is better to discuss other methods inducing charge reversal.*

**Reply P1.12.** In this article we do not consider the effect of anionic surfactants that have already been discussed, e.g. in the referenced article. Anionic surfactants indeed are used in applications listed in article introduction, although because of considerable economic constraints their application is rather limited. While we recognize the value of theoretical and applied researches on anionic surfactants, we avoided discussing them in detail to keep better focus of the scope of our article.

**Reviewer Point P1.13.** *Some figures lack tick marks on the axes. Tick marks should be added.*

**Reply P1.13.** The corresponding corrections were implemented in the text.

**Reviewer Point P1.14.** *Figs. 5-8. x-axis should be at the bottom and not be inside the graphs. The, zero-line can be added later. In some figure, the lines, symbols, and number are overlapped.*

**Reply P1.14.** The corresponding corrections were implemented in the text

**Reviewer Point P1.15.** *Table 3. The unit "mD" is not familiar to the Journal readers, I guess. It is better to replace this unit by SI unit.*

**Reply P1.15.** mD is a standard unit commonly applied in the industrial applications listed in the introduction of the article, therefore we use it in the text. However, acknowledging the reviewer's comment and multidisciplinary auditory of the journal we added conversion to SI units (Tables 1, 3, 4) as well as definition of mD unit below Table 1.

**Reviewer Point P1.16.** *Table S1. What are used surface potential as a function of pH and salt concentration for DLVO theory?*

**Reply P1.16.** The surface potential was estimated from zeta potential, according to eq. 7. The calculated values of surface potential at different pH and salinity were added to Table S2 in the supplementary materials.

**Reviewer #2:**

*This manuscript investigated the effect of pH on electrostatic interaction between hematite colloidal particles and Bentheimer sandstone, which regulates the entrapment and remobilization of the particles on porous medium. Additionally, detailed experimental characterization and theoretical study have been made to prove the credibility of results and conclusion. The employment of CT scanning technology for monitoring the migration behavior of particles provides new insight for future studies. Overall, this work is suitable for Colloids and Surfaces A, but some explanation and discussion needed to be added.*

**Reviewer Point P2.1.** *In the XRD analysis, please illustrate how to calculate the proportion of quartz and kaolinite.*

**Reply P2.1.** The XRD analysis was performed with the use of a processing software, where the proportion of the minerals is calculated as area below the corresponding peaks. The following is also stated in section 2.4.1 (page 5, lines 18-19):

‘The fractions were calculated with Bruker Diffrac.Eva software using the height of the peaks after ka2 stripping and the ratio I/I<sub>cor</sub> from the ICDD PDF-4+ 2020 database.’

**Reviewer Point P2.2.** *In section 3.3, the author presumed the change of salinity from 5000 to 0 ppm has neglectable influence on the colloidal stability. Related researches should be cited and discussed to support this statement.*

**Reply P2.2.** In general, salinity change indeed has strong influence on colloidal stability. Theoretically, the abrupt concentration raise at the propagation front of demineralized water-based hematite suspension in the rock pore channels could have caused coagulation of the particles. However, this has not been experimentally detected. In order to avoid any confusion and misunderstanding, following the comment, the text was reviewed (page 11, lines 25-29):

‘Although the initial contact of the suspension with brine could theoretically have provoked aggregation of hematite particles at the sample inlet, we did not detect any feasible indication of its occurrence. This can be explained by too little ion diffusion speed relative to the speed of the water front propagation. In any case, the possible particle flocculation at the initial phase of the test does not affect our further interpretation and conclusions regarding effect of pH increase.’

**Reviewer Point P2.3.** *In the section 3.4, the authors did not explain why the pressure change in the middle and outlet section is weaker than that of inlet section during the alteration of pH of injected water. Please explain.*

**Reply P2.3.** The following explanation was added to the section (page 14, lines 8-10):

‘The observed pressure response to the pH increase in the middle and outlet sections in both tests was much less than in the inlet section, because the most injected colloidal particles were retained at the core inlet surface or within the first section.’

**Reviewer #3:**

*The subject treated in this manuscript is practically important. However, the paper contains logically fatal point in the description with regard to the potential between macroscopic bodies. In this point major revisions are still needed.*

**Reviewer Point P3.1.** *So far, plenty of publications are reported on the deposition of colloidal particle in the porous media. It is a basis of so-called colloid facilitated transportation in the ground water and soil. Wel-known reports of Elimelech et al, have dedicated effort on the deposition process which is similar to coagulation. In this case, the approach of colloidal particles to the substrate is limited by the transportation and interaction between the substrate and particle. DLVO type for hetero-coagulation will be very useful. Analysis on the basis of potential will be very useful for the prediction of the rate of deposition.*

*On the other hand, the process of detachment is less studied. Difficulty exists that the prediction on the basis of two macroscopic bodies (particle and substrate); DLVO predict infinitely large attraction when they touch each other; the gap distance is zero. Under this situation nobody can predict the detachment by means of DLVO even though we recharge the surface by the chemical shift of pH. That is, once contact is formed, if this attraction is larger than repulsive force, they will stand for the repulsion. Nevertheless, the author concluded their result is explained by this theory. Authors are strongly requested why we can use DLVO starting from proximate contact. Expression of authors' viewpoint in this respect is necessary.*

**Reply P3.1.** We thank the reviewer for the extensive comments as well as recommendations. Some of them can be considered for implementation in future study. We also fully support the significance of the Elimelech et al results

that are referenced in our paper. However, two major points need to be clarified with regard to the research presented in our paper.

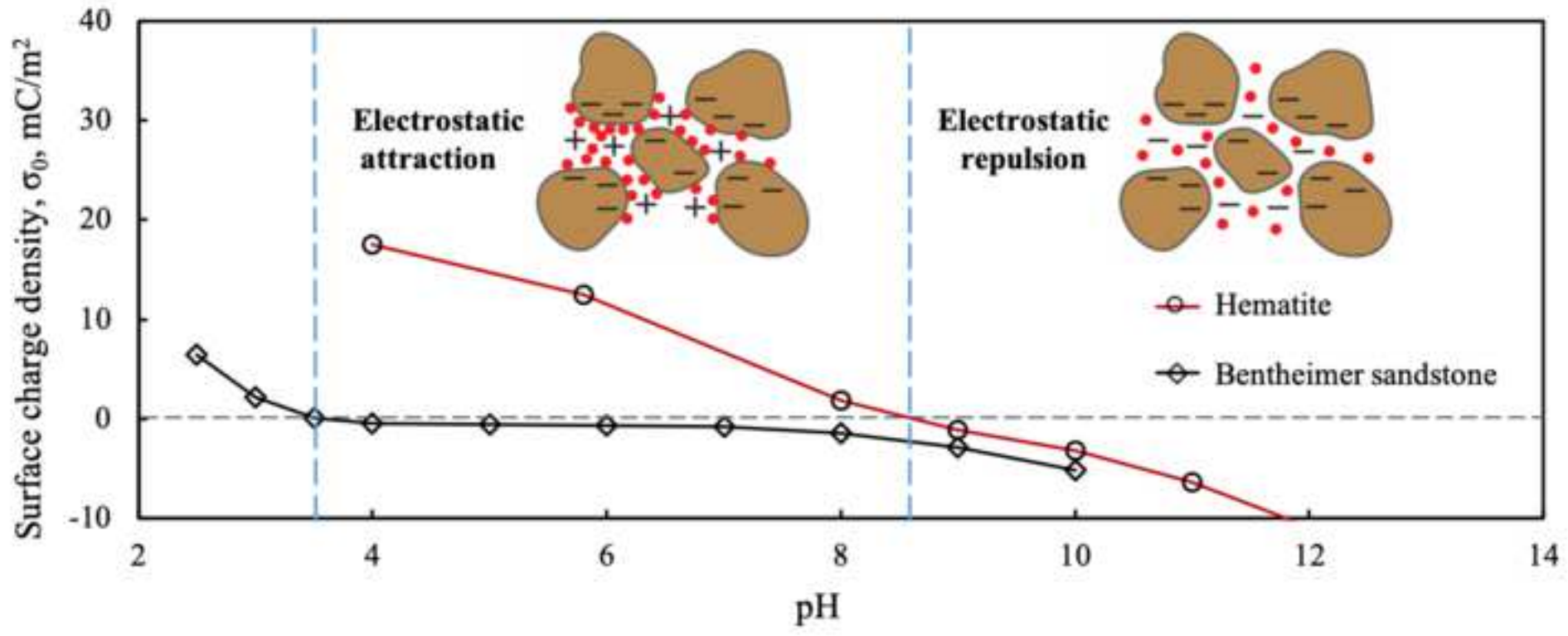
In our research, we used DLVO modelling to study the colloidal stability of hematite particles in the suspension at various pH and salinity. This was presented as a preliminary step, to explain why we inject hematite suspension in demineralized water and not in brine. Additionally the DLVO theory can be evoked to describe the interaction of the suspended particles and the pore walls.

As for detachment process of the particles, it also involves hydrodynamic drag forces. These forces will effectively mobilize the particles provided that the interaction potential has been lowered enough.

**Reviewer Point P3.2.** *One more minor issue, formation damage or permeability damage is not usual expression.*

**Reply P3.2.** *Formation damage* term is often used in the reservoir engineering domain. It means permeability reduction due to particles migration and deposition in rock porous medium. Following the reviewer's comment and acknowledging the diverse background of the journal readers, we have substituted the term *formation damage* with 'permeability impairment' or 'permeability reduction'.





# Effect of electrostatic interaction on the retention and remobilization of colloidal particles in porous media

Anna K. Kottsova<sup>a,\*</sup>, Mohsen Mirzaie Yegane<sup>b</sup>,

Alexei A. Tchistiakov<sup>a</sup>, Pacelli L.J. Zitha<sup>b</sup>

<sup>a</sup> Skoltech Center for Hydrocarbon Recovery, Skolkovo Institute of Science and Technology, Bolshoy Boulevard 30, bld. 1, Moscow, 121205, Russia

<sup>b</sup> Department of Geoscience and Engineering, Delft University of Technology, Stevinweg 1, Delft, 2628 CN, the Netherlands

\*Corresponding author. E-mail address: Anna.Kottsova@skoltech.ru

Keywords: fines, hematite particles, point of zero charge, van der Waals, electrostatic, interactions

## Abstract

We investigate the effect of pH on external hematite colloidal particles entrapment and remobilization by core-flood experiments combined with X ray computed tomography. Suspensions of calibrated hematite colloidal particles were injected into Bentheimer sandstones sample, composed mainly of well-sorted quartz and small clay fraction (up to 1 wt%), consisting mainly of kaolinite. We have found that permeability impairment due to an external cake build-up can be reversed when pH exceeds the point of zero charge of hematite particles. This effect could be successfully interpreted by the switching of the surface charge of hematite particles from positive to the negative, similar to the rock surface. The experimentally verified pH-controlled electrostatic retention and remobilization technique can be extended to other colloidal particles, having pH-dependent surface charge, including natural clay minerals in hydrocarbon and geothermal reservoirs. Therefore, varying pH of injected fluid can be applied for targeted external cake build-up and transportation of colloidal particles within a reservoir.

## 1. Introduction

Colloidal fines migration is a common phenomenon in various industrial processes relying on fluid flow in porous media, including hydrology (McDowell-Boyer et al., 1986; Torkzaban et al., 2007), geothermal engineering (Mahmoudi et al., 2010; Rosenbrand et al., 2015), gas production from hydrate-bearing sediments (Jung et al., 2012), well-bore drilling (Byrne et al., 2007; Civan, 2007), and enhanced oil recovery (EOR), where low salinity water injection emerged as a new approach to mobilize additional oil (Alshakhs & Kovscek, 2016; Iglauer et al., 2010; Nasralla et al., 2013; Pooryousefy et al., 2018; Xie et al., 2016). Water injection applied within these processes can cause impairment of permeability due to blockage of pores at the borehole walls by

1 particles, suspended in the water, or due to entrapment of migrating in-situ clay particles in pore throats within  
2 the reservoir.

3 Fines migration in porous media has been intensively investigated in the last few decades (Lei et al., 2017;  
4 Yu et al., 2019). It was established that attachment or detachment of colloidal particles from pore walls and  
5 following up their migration in porous media are determined by the balance of forces acting between the particles  
6 and the rock mineral grains surfaces. The attachment occurs thanks to London – van der Waals attraction forces.  
7 The detachment can be triggered by combined effect of repulsive forces such as the electrostatic repulsion of  
8 overlapping electrical double layers (EDL), if the surface charge of clay particles and the rock matrix has the same  
9 sign, structural forces of bound water, hydrodynamic drive of flowing fluid. (Vaidya & Fogler, 1990; Elimelech  
10 (1991, 1995); Tchistiakov, 2000; Kalantariasl & Bedrikovetsky, 2014, Kobayashi, 2005).

11 The electrostatic repulsion considerably depends on the fluid salinity as the latter changes  $\zeta$ -potentials of the  
12 interacting surfaces. The repulsion between a clay particle and a pore wall decreases with the rise of ionic strength  
13 of the pore aqueous solution and increases when the fluid salinity drops. It was experimentally demonstrated, that  
14 at low salinity of the injected fluid in-situ particles could be detached from the rock matrix surface and deposited  
15 downstream that led to significant reduction of the rock permeability (Kia et al., 1987; Vaidya & Fogler, 1990;  
16 Tchistiakov, 2000; Rosenbrand et al., 2015; Alshakhs, & Kovscek, 2016; A. Al-Sarihi et al., 2018; Borazjani et  
17 al., 2018;).

18 Besides salinity, the electrostatic interaction between clay particles and the rock mineral matrix is controlled  
19 by the pore fluid pH (Kia et al., 1987; Vaidya & Fogler, 1990, 1992; ; Mietta et al., 2009; Kobayashi et al., 2009;  
20 You et al., 2012; Kumar et al., 2017 ). It was experimentally confirmed that an increase of pH above a certain  
21 critical value causes charge reversal of natural clay  $\zeta$ -potential from positive to negative. The critical pH value,  
22 when  $\zeta$ -potential becomes zero, is called point of zero charge (Olphen H. van, 1963; Osipov V. I, 1979; Mitchell,  
23 1993). For clay particles, the point of zero charge (PZC) can vary significantly depending on their mineralogy and  
24 crystal structure, however at pH values feasible for sandstone formations it is always larger than the point of zero  
25 charge of quartz that is commonly a predominant component of the sandstones matrix (Churcher et al., 2015;  
26 Didier et al., 2015; Kosmulski, 2016; Schroth, 1997, Osipov 1979). This means that at certain pH values, in-situ  
27 clay particles as well as external colloidal particles, present in the fluid injected in the formation, can have a  
28 surface charge of the same or opposite sign with the charge of the rock pore surface. This means that we can  
29 theoretically manage migration and retention of in-situ and external colloidal particles within a reservoir porous  
30 medium by varying pH. Some research on this subject has already been done. For example Kumar et al. (2017)

1 has experimentally shown that an increase of pH causes increase of the magnitude of the long-range repulsion  
2 between a SiO<sub>2</sub> tip and a silica facet of kaolinite. The experiments were done within the range of pH above  
3 kaolinite's PZL and thus no charge reversal occurred. Kobayashi et al. (2009) have investigated the effect of pH  
4 alteration on retention of latex particles by a zirconia bed and concluded that pH increase had minor effect on the  
5 retention in comparison with salinity rise.

6 Although considerable efforts have been made to investigate the effect of pH variation on external particle  
7 migration and retention by different materials today we still do not have confident and experimentally confirmed  
8 methodology of these process management in natural reservoirs.

9 The main objective of this research was to examine the possibility of artificial management of external  
10 colloidal particles retention by natural sandstone matrix and remobilization by gradual increase of pH of the  
11 injected fluid above the mineral point of zero charge. In previous studies pressure and effluent data were mainly  
12 used for monitoring fines migration within rock porous media, in the present study next to differential pressure  
13 measurements we applied X-ray tomography for tracking the migration of remobilized particles. Hematite  
14 particles were chosen as model particles because of their pH-dependent surface charge, distinguishable red color,  
15 and high density and X-ray attenuation capacity, which make them detectable for CT-assisted core-flood  
16 experiments. Bentheimer sandstone was used as the model porous medium. Prior to core-flood experiments,  
17 characterization of the rock and particles properties was performed and colloidal stability of the hematite  
18 suspension at various ionic strength and pH was studied by the DLVO theory. For core-flood experiments, a  
19 suspension of hematite particles was injected to deposit the particles within the porous media. Thereafter,  
20 deionized water with gradually increasing pH above the IEP of hematite particles was injected to give rise to a  
21 repulsion term between particles and sandstone surface and consequently to remobilize the deposited particles.  
22 We establish theoretical and experimental conclusions that presumably can be extended to other minerals with  
23 pH-dependent surface charge, including natural minerals in porous media.

24 The paper proceeds with description of materials and methods used for the experiments, where both  
25 preparation steps and experimental methodology are illustrated. Then, the experimental results are shown,  
26 followed by the general discussion and conclusions.

## 27 **2. Materials and methods**

### 28 *2.1 Porous medium*

29 The core-flood experiments were performed with Bentheimer sandstone of Early Cretaceous age from the  
30 south-western part of the Lower Saxony Basin. Bentheimer sandstone outcrop samples are often used as model

1 natural porous medium for laboratory studies because of their lateral continuity and block scale homogeneous  
2 nature (Peksa et al., 2017). The high permeability and large pore size of Bentheimer samples make it an appealing  
3 candidate to study the migration of colloidal particles in porous media and the ensuing permeability reduction.  
4 Bentheimer sandstone, consists of more than 85% of pore throats have a size larger than 10  $\mu\text{m}$  and only 5% of  
5 them are smaller than 5  $\mu\text{m}$  (Peksa et al., 2015). Table 1 shows the physical properties of Bentheimer core samples  
6 used to conduct the core-flood experiments. After cutting and drying the cores in an oven for up to 48 hours at 60  
7  $\pm 1$   $^{\circ}\text{C}$ , the cores were placed in molds and encased in an epoxy resin to prevent bypassing the flow alongside the  
8 core. The penetration depth of the resin into the core was nearly 1.0 mm. Thereafter, the cores were precisely  
9 machined to an effective diameter of  $3.8 \pm 0.1$  cm and a length of  $17.0 \pm 0.1$  cm. The machined samples were  
10 dried for 15 hours in an oven at  $40 \pm 1$   $^{\circ}\text{C}$ . The porosities of the core samples were measured by the Helium gas  
11 expansion method. The permeability of the cores was estimated using Darcy's law, by flowing 5000 ppm NaCl  
12 brine at different rates within the core and recording the pressure drop. It should be noted that the characterization  
13 of the rock with XRD analysis and potentiometric titration measurements were performed on the rock sample  
14 pulverized to 1  $\mu\text{m}$  powder.

## 15 2.2 Chemicals

16 Hematite ( $\alpha\text{-Fe}_2\text{O}_3$  with density equal to  $5.24 \text{ g/cm}^3$ ) particles were supplied by Sigma-Aldrich in powder  
17 form with. The high density of the particles results in high attenuation of X-rays relative to quartz, the main  
18 component of the sandstone. The diameter of an individual particle was  $< 50$  nm, as reported by the manufacturer,  
19 which was obtained from BET; however, they had a strong tendency to aggregate and form larger particles,  
20 therefore in this study we further refer to them as colloidal particles. Moreover, as mentioned, hematite particles  
21 had a distinguishable red color that simplified their detection in effluent and during the microscopic examination  
22 of the sample slab after core-flood experiments. Sodium chloride (NaCl) used for brine preparation was purchased  
23 from Sigma-Aldrich as well. The base (1 M NaOH) and acid (1 M HCl) used for pH adjustment, were supplied  
24 by Merck KGaA.

25 Aqueous suspensions of hematite were used to deposit particles inside the rock porous media. Earlier studies  
26 have shown that aggregation of hematite particles increases drastically with the addition of a small quantity of  
27 salt into the aqueous solution (Dickson et al., 2012; He et al., 2008). This is supported by our analysis of the  
28 colloidal stability of hematite suspensions. Therefore, in these experiments, we use hematite suspension in  
29 ultrapure deionized water (DI water). As for initial saturation of the core, 5000 ppm NaCl brine was used to  
30 prevent clogging of pores with released in-situ clay particles before the beginning of the experiment.

### 2.3 Preparation of hematite suspension

In order to avoid air entrapment inside of the hematite aggregates and produce an air-free stable suspension of hematite particles, the following preparation procedure was applied. First, the particles were placed into a vacuum, then saturated with CO<sub>2</sub> and after secondary vacuuming mixed with deionized water and stirred (Figure 1). This was followed by sonication at the power of 550W, 20 kHz, and an amplitude of 20%. The applied procedure allowed preparing a colloidally stable suspension with no observable sedimentation. The pH of the prepared suspension was measured to be  $5.8 \pm 0.1$ . Hematite suspension of 250 ppm concentration prepared in deionized water was applied in flooding tests. During the core-flood experiments, the suspension in the tank was continuously stirred in order to maintain its homogeneity.

### 2.4 Characterization of rock and hematite particles

#### 2.4.1 XRD analysis

XRD analysis was performed to determine the composition of the rock. The XRD data were obtained on a Bruker D8 Advance diffractometer equipped with a Bragg-Brentano geometry and Lynxeye position sensitive detector and using Cu K $\alpha$  radiation. The pulverized rock was placed into an appropriate holder and its surface was made as flat as possible prior to the analysis. The scans were done with rotation on, at 45 kV and 40 mA. The measurement was performed with a coupled  $\theta$  - $2\theta$  scan with a step size of 0.025° and time per step of 2 seconds. The Semi-quantitative (S-Q) approach was used to approximate the fractions of the identified phases. The fractions were calculated with Bruker Diffrac.Eva software using the height of the peaks after ka<sub>2</sub> stripping and the ratio I/I<sub>cor</sub> from the ICDD PDF-4+ 2020 database.

#### 2.4.2 Potentiometric mass titration

The potentiometric mass titration (PMT) method was used to identify the point of zero charge (PZC) of the rock. 100 mL of 1,500 ppm NaCl (~ 0.025 mM) solution, as the background solution, was put into three different flasks. The pulverized rock with different masses of 2.5, 5.0, and 10.0 g was transferred to each flask. A blank solution without the addition of rock powder was also prepared. Before the experiment, the suspensions were stirred with a Teflon magnetic stirrer for 24 h to reach an equilibrium. Then potentiometric titrations were performed in a nitrogen atmosphere. First, 5 mL of 0.1 M NaOH was added to all flasks to deprotonate a significant portion of the surface sites, causing the surface to be negative. Next, each of these suspensions and the blank sample were titrated by addition of 0.1 M HCl to the cell in 10 – 15 steps. The samples were continuously stirred, except when the pH was recorded after every 2 – 5 min while the stirrer was switched off.

The pH-dependent surface charge density ( $\sigma_0$ ) was determined based on the measured PMT data, according to the following equation (Lützenkirchen et al., 2012):

$$\sigma_0(pH) = \frac{F \cdot (\Delta n_{sol,H^+}(pH) - \Delta n_0)}{m S_{BET}} \quad (1)$$

where  $F$  is the Faraday constant ( $F = 96500$  C/mol),  $m$  is the mass of the sample,  $S_{BET}$  is the rock specific surface area and  $\Delta n_0$  is the pH-dependent amount of acid which is consumed on a sample with a very small mass (extrapolated to zero mass). The dissolution effect ( $\Delta n_{sol,H^+}$ ) is obtained by comparison of the balance of protons ions in the potentiometric titration of suspensions with the blank potentiometric titration results according to the following equation:

$$\Delta n_{sol,H^+} = \Delta n_{acid(S)}(pH) - \Delta n_{acid(B)}(pH) \quad (2)$$

where  $\Delta n_{acid(S)}(pH)$  and  $\Delta n_{acid(B)}(pH)$  represent the balance of protons ions needed to be consumed to reach a certain pH for the suspension and blank respectively.

#### 2.4.3 Zeta potential and particle size distribution

The zeta potential and hematite particles size distribution (PSD) in deionized water were measured using a Malvern Zetasizer Nano ZS at 25 °C. Zeta potential is calculated by means of Henry's equation from the measured electrophoretic mobility. In order to enable measurements on this instrument the particles concentration was adjusted to provide a count rate of ca. 500 kcps. Samples were run in triplicate in the auto mode and the average was recorded. There was a pause of 30 – 60 sec between each run, for relaxation of the sample.

#### 2.5 Hematite inter-particle interactions

Dispersed particles are subject to Brownian motion which causes frequent inter-particle collisions. The balance between inter-particle interactions determines whether the dispersion of hematite particles is colloidally stable. According to the DLVO theory (Hotze et al., 2012; Mirzaie Yegane et al., 2020; Skoglund et al., 2013), the total energy for the interaction between two unmodified spherical particles ( $V_t$ ) with radius  $R$ , at separation distance  $h$  is given by the sum of van der Waals ( $V_v$ ) and electrostatic ( $V_e$ ) potentials:

$$V_t(x) = V_v(x) + V_e(x) \quad (3)$$

where  $x$  is the normalized separation distance equal to  $h/R$ . The van der Waals potential is (Israelachvili, 2011):

$$\frac{V_v(x)}{k_B T} = - \frac{(\sqrt{A_H} - \sqrt{A_W})^2}{6k_B T} \left\{ \frac{2}{x(x+4)} + \frac{2}{(x+2)^2} + \ln \left[ \frac{x(x+4)}{(x+2)^2} \right] \right\} \quad (4)$$

1 where  $A_H$  and  $A_W$  are Hamaker constants for hematite particle and water, as the medium, respectively (Raghavan  
 2 et al., 2000),  $k_B$  is the Boltzmann's constant and  $T$  is the absolute temperature. The electrostatic potential is  
 3 described (Oshima, 1995) by:

$$\frac{V_e(x)}{k_B T} = \frac{2\pi\epsilon_0\epsilon_r\psi_0^2 R}{k_B T} \ln[1 + \exp(-\kappa R x)] \quad (5)$$

4 where  $\epsilon_0$  is the vacuum permittivity,  $\epsilon_r$  is the medium relative permittivity,  $\psi_0$  is the surface potential and  $\kappa^{-1}$  is  
 5 Debye length which is given by:

$$\kappa^{-1} = \left( \frac{\epsilon_0\epsilon_r k_B T}{2N_A e^2 I} \right)^{0.5} \quad (6)$$

6 where  $e$  is the electronic charge,  $N_A$  is the Avogadro's number, and  $I$  is the medium ionic strength (Tadros, 2014).  
 7 Surface potential is estimated based on the zeta potential ( $\zeta$ ) using Equation 7. The Equation is obtained by  
 8 solving the Poisson–Boltzmann equation for a distribution of the point charges that decay as a function of the  
 9 radial distance from the surface of charged particle (Wijenayaka et al., 2015):

$$\psi_0 = \zeta \left( 1 + \frac{1}{\kappa R} \right) \exp(1) \quad (7)$$

10 The pH-dependent surface charge density ( $\sigma_0$ ) can be calculated according to Equations 8-9 (Plaza et al.,  
 11 2001):

$$\sigma_0 = \frac{2\epsilon_0\epsilon_r\kappa k_B T}{e} \sinh\left(\frac{e\psi_0}{2k_B T}\right) \times \left[ 1 + \frac{1}{\kappa R} F(T) + \frac{1}{(\kappa R)^2} G(T) \right]^{1/2} \quad (8)$$

$$F(T) = \frac{2}{\cos h^2\left(\frac{e\psi_0}{4k_B T}\right)}; \quad G(T) = \frac{8 \ln \left[ \cos h\left(\frac{e\psi_0}{4k_B T}\right) \right]}{\left(\frac{e\psi_0}{2k_B T}\right)} \quad (9)$$

12 Dispersions of particles stay kinetically stable if the potential barrier ( $V_{max}$ ) is larger than  $\sim 16/k_B T$  (Berg,  
 13 2010; Mirzae Yegane et al., 2020; Moskovits et al., 2005).

14 It should be noted that the terms point of zero charge and isoelectric point are often used interchangeably,  
 15 isoelectric point corresponds to the results obtained by the electrokinetic method, while the point of zero charge  
 16 value is obtained by titration (Kosmulski et al., 2016). Plaza et al. (2010). observed that for hematite particles, the  
 17 pH ( $\zeta = 0$ ) and pH ( $\psi_0 = 0$ ) are almost identical. Alvarez-Silva et al. (2010) also noted that PZC and IEP can be  
 18 considered equal if no other specific adsorption of potential-determining ions happens. To avoid confusion  
 19 between the surface potential of rock matrix surface and hematite particles, throughout this study we will refer to  
 20 this as the point of zero charge which is where the surface charge density is zero.

## 21 2.6 Core-flood experimental setup



1 The core-flood experiment setup is shown in Figure 2. The setup was placed on the couch of the CT scanner  
2 to enable monitoring of external particles migration during the core-flood experiments. A core sample was placed  
3 into a poly-ether-ether-ketone core holder, which is transparent to X-rays , and positioned in the gantry of the  
4 scanner. The core holder is oriented vertically in order to mitigate the effect of gravity on particles distribution  
5 within the injected fluid stream as well as within the core. The core holder had three differential pressure  
6 transducers (KEMA03 ATEX 1561) with  $\pm 300$  mbar range and  $\pm 1$  mbar accuracy to monitor pressure drop along  
7 the core during the experiment. Differential pressure was measured during core-flood experiments at the inlet,  
8 middle and outlet sections of the sample with lengths  $4.1 \pm 0.1$  cm,  $8.8 \pm 0.1$  cm, and  $4.0 \pm 0.1$  cm accordingly.  
9 Pressure drop over the core was also monitored using inlet and outlet pressure transducers, while the outlet  
10 pressure was set using a backpressure regulator (BPR). Fluids were injected into the core using a Quizix pump,  
11 which was operated at a constant flow rate. A fraction collector (GE Frac 920) was used for sampling the effluents  
12 at the core-holder outlet for visual detection and physical-chemical analysis of hematite particles at the outlet.

### 13 *2.7 Core-flood experimental procedure*

14 A set of core-flood experiments was performed for this study. For the discussion in the current paper we  
15 present the results of the two most representative experiments, further referred to as Experiment 1 and Experiment  
16 2. The same experimental procedure was applied to all tests. During Exp. 1, we investigated the effect of a gradual  
17 rise in pH from neutral up to pH 10 and during Exp. 2 a steeper rise from neutral to pH 12 was studied in order to  
18 investigate the effect of pH values further from PZC of hematite on the remobilization of the particles.

19 The tests were performed in three stages. First, the core sample was saturated with 5000 ppm NaCl brine and  
20 its permeability to brine was determined using Darcy's law (Darcy, 1856). Then hematite suspension in deionized  
21 water was injected at sufficiently high flow rate (25 mL/min) to prevent the gravitational segregation of the  
22 particles (Dickson et al., 2012; He et al., 2008). 60 pore volumes (PV) of hematite suspension were injected in  
23 Experiment 1, and 30 PV in Experiment 2. Lower volume injected in Exp. 2 was dictated by the significantly  
24 higher differential pressure observed during the experiment because of lower permeability of the core (as will be  
25 discussed in more detail in Section 3.4)

26 Finally, the core was subjected to the injection of deionized water at gradually increasing pH. In Exp. 1, pH  
27 steps were 7, 8, 9, 10, in the second one 7, 9, 11, and 12. The deionized water injection rate in both tests was 10  
28 mL/min. The other experimental parameters are summarized in Table 2. Before the core-flood experiments, the  
29 deionized water was passed through 0.5  $\mu\text{m}$  filter in order to prevent the effect of any solid impurities.

## 2.8 X-ray CT scanning

X-ray CT scanning was performed throughout the injection of both hematite suspension and deionized water in order to build hematite distribution profiles and track the movement of particles. Siemens SOMATOM Definition Dual Energy CT scanner with slice number of 64 slices per second and a resolution of 0.25 mm is used in this study. The scanning was performed at 140 KeV and 250 mA. To enable a quantitative analysis of hematite distribution along the core during core-flood experiments, we first established the calibration curve for CT scan number against hematite concentration by measuring the measured CT attenuation value (CT number) for hematite suspensions for solid phase concentrations ranging from 0 to 40,000 ppm. The resulting curve shown in Figure 3 show that the CT attenuation varies linearly with hematite concentration.

## 3. Results and discussion

### 3.1 Sandstone characterization

The characteristics of Bentheimer sandstone were extensively discussed in the literature (Al-Yaseri et al., 2015; Dubelaar et al., 2015; Peksa et.al 2015, 2017). Here, we only highlight the important aspects which are relevant to our study. As can be seen in Figure 4, the XRD analysis on the pulverized Bentheimer sample which was used for core-flood experiments shows, that it consists dominantly of quartz with very small fractions of kaolinite ( $99.3 \pm 0.1\text{wt}\%$  and  $0.7 \pm 0.1 \text{ wt}\%$  respectively). This is in very good agreement with observations of Farooq et al. (2011) and Al-Yaseri et al. (2015) who found that the fraction of quartz in Bentheimer sandstone is approximately 98 and 99 wt% respectively with a small fraction of kaolinite (0.5 and 0.7 wt% respectively). It should be noted that in our XRD analysis, a few very small peaks were not identified. Thus, there might be some phases present, which are not included in the fraction calculation.

The dielectric behavior of the Bentheimer sample was assessed based on the alteration in surface charge as a result of the change in the pH. The surface charge of silica, as the main component of the Bentheimer sandstone, is due to adsorption or dissociation of protons on the surface and the consequent ionization of the silanol groups represented by the following reactions (Davis et al., 1978; Lecourtier et al., 1990):



Based on the PMT method, the point of zero charge (PZC) of the Bentheimer sample was found to be  $3.4 \pm 0.1$  (see Figure S1 in the supplementary materials). This is in agreement with the finding of Farooq et al. (2011) who also used the PMT method and whose Bentheimer sample had a quartz fraction of approximately 98 wt%.

1 However, the value of PZC measured in this study differs from the observation of Peksa et al. (2015) whose  
2 Bentheimer sample had a quartz fraction of approximately 92 wt% and measured a PZC of nearly 8. They  
3 attributed this unexpected high PZC to the presence of clay (~ 2.7 wt%) and iron particles (0.2 wt%) distributed  
4 in the sample. Further work on this matter is not within the scope of this study. Figure 5 indicates the surface  
5 charge density and proton balance related to the dissolution effects based on the PMT data. Above the PZC, the  
6 sandstone surface was dominated by  $\text{SiO}^-$  sites and as a result, it became negatively charged. The magnitude of  
7 negative surface charge density increases with increasing pH due to the dissociation of silanol groups. Such an  
8 increase is more pronounced at  $\text{pH} > 7$ . Lecourtier and Chauveteau (1990) cautioned interpreting the data at  $\text{pH}$   
9  $> 7$  because of possible silica dissolution. Nonetheless, it is generally accepted that with increasing pH beyond  
10 the PZC, more and more negative charges become available on the sandstone surface. The estimated values for  
11 the surface charge density in this study were in good agreement with the observation of Behrens and Grier (2001)  
12 who estimated the surface charge density of a silica sample.

### 13 *3.2 Colloidal stability of hematite particles*

14 To study the colloidal stability of hematite particles, first, their zeta potential at various pH was measured in  
15 a medium with very low ionic strength ( $I = 1 \text{ mM}$ , equivalent to 60 ppm NaCl). As shown in Figure 6, , the PZC  
16 of hematite particles was approximately 8.5 in good agreement with measurements reported by others (Kosmulski  
17 et al., 2016; Plaza et al., 2010). At pH values above the PZC, the zeta potential values of the particles became  
18 more negative, reaching values close to  $-22 \text{ mV}$  at pH 12. The measured zeta potential and PZC of the hematite  
19 particles agree well with values reported in the literature (He et al., 2008; Kosmulski, 2002, 2006; Nattich-Rak et  
20 al., 2012; Xu et al., 2015; Zhou et al., 2014).

21 The relative contributions of the surface forces to particles interactions were predicted by estimating the van  
22 der Waals and electrostatic potentials using the DLVO theory (see Section 2.5). Moreover, as will be seen below,  
23 the calculations provide insights needed to choose an appropriate ionic strength and pH for the hematite  
24 suspension used in the core-floods . For this purpose, the colloidal stability of hematite particles was studied by  
25 varying (a) ionic strength and (b) pH. As shown in Equation 4, to estimate the van der Waals potential, the  
26 Hamaker constant for hematite ( $A_H$ ) must be known. The Hamaker constant for hematite particles interacting with  
27 each other across the water, as the medium, can be calculated from the Lifshitz theory, assuming small differences  
28 in dielectric and magnetic properties (Faure et al., 2011). A Hamaker constant of  $25 \times 10^{-20} \text{ J}$  was used for the  
29 DLVO calculations in this study (Rohem Peçanha et al., 2019). The list of other parameters used in the calculations  
30 is given in Table S1 in the supplementary materials.

1 Figure 7a shows the total inter-particle interaction potential as a function of particle separation distance for  
2 hematite particles at pH 5.8 by varying the ionic strength. At very low ionic strength ( $I = 1$  mM), the potential  
3 barrier was approximately  $110/k_B T$ . This implies that colloidal stability is ensured. Nonetheless, increasing the  
4 ionic strength to 50, 85 and 200 mM led to a potential barrier smaller than  $16/k_B T$  implying that the colloidal  
5 stability is not achieved. It should be noted that  $I = 85$  mM is equivalent to 5,000 ppm NaCl solution which is  
6 used to saturate the core prior to injection of hematite suspension.

7 The effect of pH on the colloidal stability of hematite particles was investigated by varying the pH from 4 to  
8 12. As can be seen in Figure 7b, for pH 4, 5.8, and 12 the potential barrier is larger than  $16/k_B T$ ; however, for  
9 pH 8 and 10 the potential barrier was found to be smaller than  $16/k_B T$ . This is attributed to the density of charges  
10 on the surface of hematite particles. At pH close to the PZC of hematite particles, the density of charges is low  
11 and the van der Waals potential is dominant over the electrostatic potential. Nonetheless, at pH far away from  
12 PZC, as it is also evident from zeta potential measurements, the charges density is high enough to make the  
13 electrostatic potential larger than the van der Waals potential. This ensures the colloidal stability of hematite  
14 particles. The change in colloidal stability as a function of pH is also noticeable from visual inspection and PSD  
15 measurement (see Figure S2 and S3 in the supplementary materials which shows the suspension of hematite  
16 particles at various pH and their PSD respectively) and only the suspensions with pH far away from the PZC are  
17 colloidally stable.

### 18 3.3 Deposition of hematite particles in porous media

19 Based on the results of the above analysis of stability of the suspension of hematite colloidal particles, we  
20 chose to work with hematite particles dispersed in deionized water at pH 5.8 as it indicated sufficient colloidal  
21 stability. As hematite particles have a strong tendency to aggregate and form larger particles even in a very short  
22 time scale (He et al., 2008), the suspension was continuously stirred prior to injection to the core.

23 We injected suspensions with hematite concentration of 250 ppm in deionized water into the core which was  
24 saturated with 5000 ppm NaCl solution. It should be noted that with such approach pH and salinity are changed  
25 simultaneously. Although the initial contact of the suspension with brine could theoretically have provoked  
26 aggregation of hematite particles at the sample inlet, we did not detect any feasible indication of its occurrence.  
27 This can be explained by too little ion diffusion speed relative to the speed of the water front propagation. In any  
28 case, the possible particle flocculation at the initial phase of the test does not affect our further interpretation and  
29 conclusions regarding the effect of pH increase.

1 The estimated charge density shown in Figure 8 reveals that in the pH ranging from  $3.4 \pm 0.1$  to  $8.5 \pm 0.1$ , the  
2 hematite and rock surface have opposite charges and consequently their interaction between the particles and rock  
3 surface is dominated by electrostatic attraction whereas at  $\text{pH} > 8.5 \pm 0.1$  it is mainly by electrostatic repulsion.  
4 Therefore, by the injection of deionized water-based suspension with pH 5.8, the interaction between particles  
5 and pore walls can be expected to be dominated by an electrostatic attraction.

6 Flooding with deionized water-based suspension triggered predictable in-situ clay particles detachment and  
7 migration due to salinity drop. Even though clay represented only less than 1 wt% of the dry sandstone, their  
8 presence was visually detected in the effluent as a turbidity, sampled during the first 2 PV injected (see Figure S4  
9 in the supplementary materials). Since the transparency of the effluent was restored upon injection of 5 PV, for  
10 the overall interpretation of the experiments we consider that such low clay content does not influence the results  
11 of the study.

12 In our experiments, it was observed that hematite nanoparticles affect permeability mainly in the porous  
13 medium near the inlet of the samples. Figure 9 shows the differential pressures obtained in Exp. 1. The differential  
14 pressure in the first section rose above other sections consistently with the build-up of a filter cake due to a higher  
15 amount of particles retained and then increased almost linearly. The filter cake observed at the core inlet after the  
16 experiments is shown in Figure 10. On the other hand, a successively smaller permeability decrease was observed  
17 in the middle and outlet section of the cores. Upon injection of 32 PV in Exp. 1 and 14 PV in the second one,  
18 hematite particles appeared in the effluent (see Figure S4 in the supplementary material). Their concentration in  
19 the effluent consistently increased in both tests until the end of hematite suspension injection (60 PV in  
20 Experiment 1 and 30PV in the second). Different time of filter cake build-up and particles penetration to the outlet  
21 is attributed to the difference in the core properties, permeability in particular.

22 The formation of the external filter cake could occur due to electrostatic retention of positively charged  
23 hematite particles by negatively charged quartz matrix. Although at later stages of deposition, when quartz surfaces  
24 got considerably covered by hematite particles, they could produce lateral repulsion effects (Kobayashi et al.,  
25 2014) screening the electrostatic attraction of quartz surfaces. At this stage size-exclusion interception of hematite  
26 micro-aggregates, formed in the suspension, could become dominant. It is believed that size-exclusion occurs if  
27 infiltrated fines size exceeds  $1/6$  of the mean pore diameter (Civan, 2016). The contact of deionized water-based  
28 suspension with NaCl brine during its initial displacement could contribute to the aggregation of hematite particles  
29 at the core inlet. However, ion diffusion speed was theoretically predicted to be several orders of magnitude lower

1 than the speed of concentration front propagation into the core and in our opinion this effect has negligible  
2 influence on the results of our study.

3 Analysis of CT-derived hematite concentration along the core during the suspension injection confirmed  
4 gradual propagation of the particles through the core, although their maximum concentration occurred within the  
5 external filter cake at the inlet surface of the cores (Figure 11). At the horizontal axis of the graph, zero coordinate  
6 corresponds to the inlet surface of the sample, negative coordinates correspond to the accumulating external filter  
7 cake, and positive coordinates correspond to measurements within the core. The CT-derived particles distribution  
8 along the samples was in agreement with high-resolution images of the sample slab along its length, made upon  
9 completing the flooding tests (Figure 12). Saturation of the reddish color, the characteristic of hematite particles,  
10 was maximum at the inlet side (left) of the cores and gradually decreased towards their outlet sides (right).

### 11 *3.4 Mobilization of hematite fine particles by pH increase*

12 Upon completing the injection of the hematite suspension, the core was subjected to flooding with deionized  
13 water of increasingly higher pH to initiate hematite particles transport inside the porous medium. The change in  
14 differential pressure upon switching from suspension to deionized water observed in Figure 9 was caused by the  
15 reduction of the flow rate from 25 mL/min to 10 mL/min. In Exp. 1, the flooding with water with the pH increasing  
16 from 7 to 9 caused a gradual rise of differential pressure and consequent decrease of permeability within the inlet  
17 sections. In Exp. 2, the rise of differential pressure at same pH levels was noticeably higher. Slight differential  
18 pressure rise was also observed within the middle and outlet sections during Exp. 2. The build-up of the differential  
19 pressure in the inlet sections is believed to be mainly caused by compaction of the filter cake under the  
20 hydrodynamic pressure as well as possible partial flushing particles into the rock and increased clogging of pore  
21 throats within the core inlet section. The more pronounced pressure raise in the middle and outlet sections of the  
22 second core can be attributed to either penetration of hematite particles or migration of in-situ clays that may  
23 disperse from sand grains due to treatment with low concentrated NaOH, that was used for adjusting the pH of  
24 the fluids (Osipov 1979).

25 The increase of the injected water pH from 9 to 10 in Experiment 1 resulted in differential pressure decline  
26 within the inlet section. The differential pressure continuously decreased during the injection of the first 5 PV and  
27 stabilized upon the injection of 6 PV (Figure 9). Differential pressure in the middle and outlet section of the core,  
28 on the other hand, started slightly rising after 5 PV injected. However, in both tests no hematite presence was

1 detected in the effluent, meaning that all released particles were still retained within the core even after the  
2 injection of a large number of PVs.

3 Further increase in the pH of the injected deionized water from 9 to 11 in Exp. 2 resulted in a steep decrease  
4 in the differential pressure drop in the inlet section of the core (Figure 9). Pressure in the middle and outlet sections  
5 remained unchanged. Further increase of pH from 11 to 12 resulted in a consistent decline of the differential  
6 pressure in the inlet section and a much less pronounced rise of differential pressure in the middle and outlet  
7 sections of the core. The differential pressure decline in the inlet section persisted even upon injection of 10 PV  
8 while rising asymptotically to a final value in the middle and outlet sections. The observed pressure response to  
9 the pH increase in the middle and outlet sections in both tests was much less than in the inlet section, because the  
10 most injected colloidal particles were retained at the core inlet surface or within the first section.

11 The concentration of particles inside the core was monitored at different stages of both tests with CT-scan.  
12 Analysis of the CT-data showed that up to the PZC of hematite particles, the signal from the filter cake was  
13 increasing (see Figure S5 in supplementary materials). This is in agreement with differential pressure data that  
14 indicated consolidation of the filter cake under the hydrodynamic force. After pH increased above the PZC CT-  
15 derived concentration profiles confirmed the decrease of particle concentration in the inlet core section. It should  
16 be mentioned that care must be taken to minimize unavoidable artifacts associated with CT scanning to perform  
17 reliable quantitative analysis.

#### 18 **4. General discussion**

19 The purpose of this work was to study the effect of pH alteration on entrapment and remobilization of  
20 hematite colloidal particles in porous media. We investigated the charge reversal of the particles above their point  
21 of zero charge as a technique to remobilize the deposited particles and transport them in porous media.

22 The retention of particles and their further transport was primarily observed by the differential pressure  
23 measurements at different lengths of the core. During the hematite deposition stage, the pressure data suggested  
24 subsequent deposition of the particles in all sections of the core and formation of a filter cake in the inlet section.  
25 Injection of deionized water with pH lower than the point of zero charge of hematite particles (i.e.  $\text{pH } 8.5 \pm 0.1$ )  
26 did not trigger any particles migration as the electrostatic interaction between positively charged hematite particles  
27 and negatively charged quartz grains of the rock matrix surface was attractive. Injection of deionized water at pH  
28 9, which is slightly above the point of zero charge of hematite particles, also did not cause particles mobilization  
29 suggesting that the density of negative charges on the particles surface was not high enough to ensure an adequate  
30 electrostatic repulsion between particles and rock matrix surface that cause detachment of particles (see Figure 8

1 for surface charge density of hematite particles and rock matrix at various pH). Increasing pH to 10, however, led  
2 to a decrease of differential pressure in the inlet section and its build-up downstream, indicating the start of the  
3 migration of the particles from the inlet surface further inside the core. Further increase in pH, according to the  
4 surface charge measurements, led to giving rise to a larger electrostatic repulsion term due to the increase of  
5 surface charge density of both hematite and quartz particles. The increase in surface charge density could also  
6 contribute to the deflocculation of hematite aggregates formed at the core inlet and penetration of the dispersed  
7 particles into the rock. However, the permeability restoration occurred only partially which suggests that the size-  
8 exclusion retention of the coagulated hematite particles remained, while the electrostatic retention was eliminated.  
9 Analysis of the CT-derived concentration profiles of the hematite also showed the migration of the particles  
10 associated with increasing pH.

11 The observed results prove the premise that above the point of zero charge, hematite particles came into  
12 repulsive interaction with the rock matrix surface which resulted in their detachment and further penetration into  
13 the core. However, we found that apart from the sign, the density of charges also plays an important role and at  
14 pH values higher but close to the point of zero charge, the density of negative charges on the surface of particles  
15 was too small to cause their remobilization.

16 The discussed hypothesis was previously reviewed in several studies. In the work of Vaidya and Fogler  
17 (1992) migration of in-situ kaolinite particles was observed as a function of pH and severe permeability  
18 impairment was observed after the charge reversal of the particles due to particles mobilization. A more recent  
19 work of Mahmoudi et al. (2016) also observed kaolinite migration in the sandstone at high pH values. In both  
20 these studies change of salinity and pH conditions were performed and observed simultaneously whereas in our  
21 study we analyzed the influence of pH only. Generally, our work is in agreement with the aforementioned studies  
22 on the hypothesis of mobilization of particles with a pH-dependent surface charge at a high pH level. As the step  
23 forward in the ongoing research we provide a detailed theoretical study of colloidal stability of hematite particles  
24 and report the effect of surface charge density of particles and rock matrix on the electrostatic interaction between  
25 them. Moreover, we experimentally established the theoretical possibility of external particles remobilization and  
26 migration because of their charge reversal caused by pH increase, by means of variety of methods, including CT  
27 scanning technique that proved to be an effective tool for monitoring the migration of colloidal particles in the  
28 porous media throughout the experiment.

29 The following limitations of this work must be acknowledged. The strong tendency of hematite colloidal  
30 particles to aggregate needs to be taken into account in all stages of the particles characterization and core-flood



1 experiments. For instance, particles tend to sediment shortly after preparation, therefore the analysis of their  
2 particle size distribution, determined by dynamic light scattering, should be done with caution. Besides,  
3 limitations of CT scanning include minimization of experimental artifacts for the quantitative analysis. These  
4 artifacts can appear on CT images as an effect of the core position inside the scanner and selected scanning  
5 parameters and they need to be minimized at the preparation stage and during image analysis. Also, the  
6 interpretation of the core-flood experiments in our study was primarily focused on the interactions between  
7 particles and rock surface. Further theoretical studies which include both rock-particle and particle-particle  
8 interactions are recommended.

9 As mentioned before, hematite particles were chosen for the study specifically because they have pH-  
10 dependent surface charge and are traceable under CT scan. However, we believe that the conclusions of this study  
11 can be extrapolated to real field-case applications of natural clastic reservoirs. The main mineral of such reservoirs  
12 is quartz, similar to the rock in our studies. Since the point of zero charge of quartz is lower than the naturally  
13 occurring pH, the sand grains surfaces are usually negatively charged in clastic reservoirs. Clay minerals, usually  
14 presented in the natural rocks, have very different and complex mineralogy and crystal structure, therefore their  
15 PZC can vary significantly. At the same time clay minerals, similar to colloidal particles of hematite used in this  
16 study, are hydrated in water and therefore respond to the changes in the surrounding environment. At naturally  
17 occurring pH clay particles are electrostatically attracted to quartz grains and an increase in pH can reverse their  
18 surface charge and initiate migration, as it was shown in the works mentioned above (Mahmoudi et al., 2016;  
19 Vaidya & Fogler, 1992). Therefore, we suggest that the mechanism of particle charge reversal due to an increase  
20 of pH over the PZC can result in the same behavior for clay minerals in the natural clastic rocks and other minerals  
21 with pH-dependent surface charge. This suggestion is a foundation for further detailed and comparative research.

## 22 **5. Conclusions**

23 In this work, the impact of pH alteration on entrapment and remobilization of hematite particles in a sandstone  
24 porous medium was investigated. The experiments showed that the rock surface was negatively charged at pH  
25 values higher than ~3.4 while the surface of hematite particles became negatively charged only at pH values  
26 higher than ~8.5. Injection of the hematite suspension at original pH 5.8 into the sandstone core led to the  
27 formation of a filter cake in the inlet due to the combined effect of electrostatic retention of positively charged  
28 hematite particles on negatively rock surface and size-exclusion interception of hematite micro-aggregates formed  
29 in the suspension. During the injection of deionized water with pH values up to 9, no indication of hematite  
30 particles mobilization in the filter cake was observed. At pH values higher than 9, however, a decrease of

1 differential pressure in the inlet section was noticed, indicating the start of the migration of the particles from the  
2 inlet surface further inside the core and partial destruction of the filter cake. This was due to a change of surface  
3 charge of hematite particles from positive to negative giving rise to a repulsion term when they interact with  
4 negatively charged rock surface which ceases electrostatic retention of hematite particles and enables their further  
5 penetration into the rock porous network. Analysis of the CT-derived concentration profiles also showed the  
6 decrease of particle concentration in the inlet core section at pH values higher than 9. The results of this study  
7 provide insights into fine-tuning the electrostatic interactions in porous media and thus mitigating the permeability  
8 reduction as a result of fines migration for particles with pH-dependent surface charge.

### 9 **Acknowledgements**

10 This work was supported by the Ministry of Science and Higher Education of the Russian Federation  
11 under agreement No. 075-15-2020-119 within the framework of the development program for a world-class  
12 Research Center. We thank the Ministry of Science and Higher Education of the Russian Federation for its  
13 support.

14 The authors gratefully acknowledge the Skolkovo Institute of Science and Technology (Russia) and Delft  
15 University of Technology (The Netherlands) for providing their laboratories facilities for the experiments. The  
16 authors thank Michiel Slob, Jolanda van Haagen, Marc Friebe, and Ellen Meijvogel-de Koning for technical  
17 support. The authors also acknowledge Martijn Janssen, Swej Shah, and Sian Jones for fruitful discussions.

1 **References**

- 2 1. Aji, K., You, Z., Badalyan, A., & Bedrikovetsky, P. (2012). Study of particle straining effect on produced  
3 qater management and injectivity enhancement. *SPE International Production and Operations Conference  
4 and Exhibition, Doha Qatar*, (May), 14–16.
- 5 2. Al-Sarihi, A., Zeinijahromi, A., Genolet, L., Behr, A., Kowollik, P., & Bedrikovetsky, P. (2018). Effects of  
6 Fines Migration on Residual Oil during Low-Salinity Waterflooding. *Energy & Fuels*, 32(8), 8296-8309.  
7 doi:10.1021/acs.energyfuels.8b01732
- 8 3. Al-Yaseri, A. Z.; Lebedev, M.; Vogt, S. J.; Johns, M. L.; Barifcani, A.; Iglauer, S. (2015) Pore-scale analysis  
9 of formation damage in Bentheimer sandstone with in-situ NMR and micro-computed tomography  
10 experiments. *Journal of Petroleum Science and Engineering*, 129, 48-57.
- 11 4. Alexandrino, J. S., Peres, A. E. C., Lopes, G. M., & Rodrigues, O. M. S. (2016). Dispersion degree and zeta  
12 potential of hematite. *Revista Escola de Minas*, 69(2), 193–198. [https://doi.org/10.1590/0370-  
13 44672014690073](https://doi.org/10.1590/0370-44672014690073).
- 14 5. Alshakhs, M. J., & Kovscek, A. R. (2016). Understanding the role of brine ionic composition on oil recovery  
15 by assessment of wettability from colloidal forces. *Advances in Colloid and Interface Science*, 233, 126-  
16 138. doi:<https://doi.org/10.1016/j.cis.2015.08.004>
- 17 6. Alvarez-Silva, M., Mirnezami, M., Uribe-Salas, A., & Finch, J. A. (2010). Point of Zero Charge , Isoelectric  
18 Point and Aggregation of Phyllosilicate Minerals. *Canadian Metallurgical Quaterly*, 49, 405–410.  
19 <https://doi.org/10.1179/cmq.2010.49.4.405>.
- 20 7. Austad, T.; RezaeiDoust, A.; Puntervold, T. (2010). Chemical mechanism of low salinity water  
21 flooding in sandstone reservoirs. *SPE improved oil recovery symposium; Society of Petroleum Engineers:*  
22 Richardson, TX, USA; DOI: 10.2118/129767-MS.
- 23 8. Barouch, E., Wright, T. H., & Matijević, E. (1987). Kinetics of particle detachment: I. General  
24 considerations. *Journal of Colloid and Interface Science*, 118(2), 473-481. doi:[https://doi.org/10.1016/0021-  
25 9797\(87\)90483-8](https://doi.org/10.1016/0021-9797(87)90483-8)
- 26 9. Behrens, S. H.; Grier, D. G. (2001). The charge of glass and silica surfaces. *The Journal of Chemical Physics*,  
27 115, (14), 6716-6721.
- 28 10. Berg, J. C. (2010). *An Introduction to Interfaces & Colloids the Bridge to Nanoscience;* World Scientific  
29 Publishing Co. Pte. Ltd: Singapore.

- 1 11. Borazjani, S., Kulikowski, D., Amrouch, K., & Bedrikovetsky, P. (2018). Composition changes of  
2 hydrocarbons during secondary petroleum migration. *The APPEA Journal*, 58, 784. doi:10.1071/AJ17127
- 3 12. Byrne, M., Patey, I., & Green, J. (2007). A New Tool for Exploration and Appraisal-Formation Damage  
4 Evaluation.
- 5 13. Churcher, P. L., French, P. R., Shaw, J. C., & Schramm, L. L. (1991). Rock Properties of Berea Sandstone,  
6 Baker Dolomite, and Indiana Limestone. *SPE International Symposium on Oilfield Chemistry, Anaheim,*  
7 *California*, (January), 431–446. <https://doi.org/10.2118/21044-MS>
- 8 14. Civan F. (2016) *Reservoir Formation Damage. 3rd edition.* Elsevier Inc.  
9 <https://doi.org/10.1016/B978-0-12-801898-9.00028-X>
- 10 15. Dahneke, B. (1975). Resuspension of particles. *Journal of Colloid and Interface Science*, 50(1), 194-196.  
11 doi:[https://doi.org/10.1016/0021-9797\(75\)90266-0](https://doi.org/10.1016/0021-9797(75)90266-0)
- 12 16. Darcy, H. (1856). *Les Fontaines Publiques de la Ville de Dijon*, Dalmont, Paris.
- 13 17. Davis, J. A.; James, R. O.; Leckie, J. O. (1978). Surface ionization and complexation at the oxide/water  
14 interface: I. Computation of electrical double layer properties in simple electrolytes. *Journal of Colloid and*  
15 *Interface Science*, 63, (3), 480-499.
- 16 18. Dickson, D., Liu, G., Li, C., Tachiev, G., & Cai, Y. (2012). Dispersion and stability of bare hematite  
17 nanoparticles: effect of dispersion tools, nanoparticle concentration, humic acid and ionic strength. *Science*  
18 *of the Total Environment*, 419, 170–177. <https://doi.org/10.1016/j.scitotenv.2012.01.012>.
- 19 19. Didier, M., Chaumont, A., Joubert, T., Bondino, I., & Hamon, G. (2015). Contradictory trends for smart  
20 water injection method: role of pH and salinity from sand/oil/brine adhesion maps. *International Symposium*  
21 *of the Society of Core Analysts*, 12.
- 22 20. Elimelech, M., Gregory, J., Xia, X., Williams, R.A. (1995). *Particle Deposition and Aggregation*, paperback  
23 ed., Butterworth-Heinemann, Oxford.
- 24 21. Elimelech, M. (1991). Kinetics of capture of colloidal particles in packed beds under attractive double layer  
25 interactions, *J. Colloid Interf. Sci.* 146, 337–352.
- 26 22. Farooq, U.; Tweheyo, M. T.; Sjöblom, J.; Øye, G. (2011) Surface Characterization of Model, Outcrop, and  
27 Reservoir Samples in Low Salinity Aqueous Solutions. *Journal of Dispersion Science and Technology*, 32,  
28 (4), 519-531.
- 29 23. Faure, B.; Salazar-Alvarez, G.; Bergström, L. (2011). Hamaker Constants of Iron Oxide Nanoparticles.  
30 *Langmuir*, 27, (14), 8659-8664.

- 1 24. He, Y. T., Wan, A. J., & Tokunaga, At. (2008). Kinetic stability of hematite nanoparticles : the effect of  
2 particle sizes. *The Journal of Nanoparticle Research*, 10, 321–332. [https://doi.org/10.1007/s11051-007-](https://doi.org/10.1007/s11051-007-9255-1)  
3 9255-1
- 4 25. Hotze, E. M.; Phenrat, T.; Lowry, G. V. (2010). Nanoparticle aggregation: challenges to understanding  
5 transport and reactivity in the environment. *J Environ Qual*, 39, (6), 1909-24.
- 6 26. Iglauer, S., Favretto, S., Spinelli, G., Schena, G., & Blunt, M. J. (2010). X-ray tomography measurements  
7 of power-law cluster size distributions for the nonwetting phase in sandstones. *Phys Rev E Stat Nonlin Soft*  
8 *Matter Phys*, 82(5 Pt 2), 056315. doi:10.1103/PhysRevE.82.056315
- 9 27. Israelachvili, J. (2011). *Intermolecular and Surface Forces 3rd Edition*. Academic Press.
- 10 28. Jung, J. W., Jang, J., Santamarina, J. C., Tsouris, C., Phelps, T. J., & Rawn, C. J. (2012). Gas Production  
11 from Hydrate-Bearing Sediments: The Role of Fine Particles. *Energy & Fuels*, 26(1), 480-487.  
12 doi:10.1021/ef101651b
- 13 29. Kalantariasl, A., & Bedrikovetsky, P. (2014). Stabilization of External Filter Cake by Colloidal Forces in a  
14 “Well–Reservoir” System. *Industrial & Engineering Chemistry Research*, 53(2), 930-944.  
15 doi:10.1021/ie402812y
- 16 30. Katende, A., & Sagala, F. (2019). A critical review of low salinity water flooding: Mechanism, laboratory  
17 and field application. *Journal of Molecular Liquids*, 278, 627–649.  
18 <https://doi.org/10.1016/j.molliq.2019.01.037>
- 19 31. Kia, S. F., Fogler, H. S., & Reed, M. G. (1987). Effect of pH on colloiddally induced fines migration. *Journal*  
20 *of Colloid and Interface Science*, 118(1), 158-168. doi:[https://doi.org/10.1016/0021-9797\(87\)90444-9](https://doi.org/10.1016/0021-9797(87)90444-9)
- 21 32. Kia, S. F., Fogler, H. S., Reed, M. G., & Vaidya, R. N. (1987). Effect of Salt Composition on Clay Release  
22 in Berea Sandstones. *SPE Production Engineering*, 2(04), 277-283. doi:10.2118/15318-PA
- 23 33. Kobayashi, M., Nanaumi, H., Muto, Y. (2009). Initial deposition rate of latex particles in the packed bed of  
24 zirconia beads. *Colloids and Surfaces A: Physicochem. Eng. Aspects*, 347, 2-7.
- 25 34. Kobayashi, M., Ookawa, M., Yamada, S. (2014) The effects of surface charging properties on colloid  
26 transport in porous media. *Applied Mechanics J.*, vol.17, 743-752.
- 27 35. Kolakowski, J. E., & Matijević, E. (1979). Particle adhesion and removal in model systems. Part 1.—  
28 Monodispersed chromium hydroxide on glass. *Journal of the Chemical Society, Faraday Transactions 1:*  
29 *Physical Chemistry in Condensed Phases*, 75(0), 65-78. doi:10.1039/F19797500065

- 1 36. Kosmulski, M. (2002) The pH-Dependent Surface Charging and the Points of Zero Charge. *Journal of*  
2 *Colloid and Interface Science*, 253, (1), 77-87.
- 3 37. Kosmulski, M. (2006). pH-dependent surface charging and points of zero charge III. Update. *Journal of*  
4 *Colloid and Interface Science*, 298, (2), 730-41.
- 5 38. Kosmulski, M. (2016). Isoelectric points and points of zero charge of metal (hydr)oxides : 50 years after  
6 Parks' review. *Advances in Colloid and Interface Science*, 238, 1–61.  
7 <https://doi.org/10.1016/j.cis.2016.10.005>
- 8 39. Kumar, N., Andersson, M. P., van den Ende, D., Mugele, F., & Siretanu, I. (2017). Probing the Surface  
9 Charge on the Basal Planes of Kaolinite Particles with High-Resolution Atomic Force Microscopy.  
10 *Langmuir*, 33(50), 14226-14237. doi:10.1021/acs.langmuir.7b03153
- 11 40. Lei, H., Dong, L., Ruan, C., & Ren, L. (2017). Study of migration and deposition of micro particles in porous  
12 media by Lattice-Boltzmann Method. *Energy Procedia*, 142, 4004-4009.  
13 doi:<https://doi.org/10.1016/j.egypro.2017.12.317>
- 14 41. Lecourtier, J.; Lee, L. T.; Chauveteau, G. (1990). Adsorption of polyacrylamides on siliceous minerals.  
15 *Colloids and Surfaces*, 47, 219-231.
- 16 42. Lützenkirchen, J.; Preocanin, T.; Kovačević, D.; Tomišić, V.; Lövgren, L.; Kallay, N. (2012). Potentiometric  
17 Titrations as a Tool for Surface Charge Determination. *Croatica Chemica Acta*, 85, 391-417.
- 18 43. Mahmoudi, M., Fattahpour, V., Nouri, A., & Leitch, M. (2016). An Experimental Investigation of the Effect  
19 of pH and Salinity on Sand Control performance for heavy oil thermal production. *SPE Canada Heavy II*  
20 *Technical Conference, Calgary*, (June), 18. <https://doi.org/10.2118/180756-MS>
- 21 44. McDowell-Boyer, L. M., Hunt, J. R., & Sitar, N. (1986). Particle transport through porous media. *Water*  
22 *Resources Research*, 22(13), 1901-1921. doi:10.1029/WR022i013p01901
- 23 45. Mietta, F., Chassagne, C., & Winterwerp, J. C. (2009). Shear-induced flocculation of a suspension of  
24 kaolinite as function of pH and salt concentration. *Journal of Colloid and Interface Science*, 336(1), 134-  
25 141. doi:<https://doi.org/10.1016/j.jcis.2009.03.044>
- 26 46. Mirzaie Yegane, M.; Minaye Hashemi, F. S.; Vercauteren, F.; Meulendijks, N.; Gharbi, R.; Boukany, P. E.;  
27 Zitha, P. L. J. (2020). Rheological response of a modified polyacrylamide – silica nanoparticles hybrid at  
28 high salinity and temperature. *Soft Matter*, 16, 10198-10210. doi:[10.1039/d0sm01254h](https://doi.org/10.1039/d0sm01254h)
- 29 47. Mitchell, J. K. (1993). *Fundamentals of Soil Behavior*. John Wiley & Sons, Inc.
- 30 48. Moskovits, M.; Vlčková, B. (2005). Adsorbate-Induced Silver Nanoparticle Aggregation Kinetics. *The*

- 1 *Journal of Physical Chemistry B*, 109, (31), 14755-14758.
- 2 49. Nasralla, R. A., Bataweel, M. A., & Nasr-El-Din, H. A. (2013). Investigation of Wettability Alteration and  
3 Oil-Recovery Improvement by Low-Salinity Water in Sandstone Rock. *Journal of Canadian Petroleum*  
4 *Technology*, 52(02), 144-154. doi:10.2118/146322-PA
- 5 50. Ohshima, H. (1995). Effective Surface Potential and Double-Layer Interaction of Nanoparticles. *Journal of*  
6 *Colloid and Interface Science*, 174, (1), 45-52.
- 7 51. Olphen H. van., (1963). *An introduction to clay colloid chemistry*. Interscience Publications (New York).
- 8 52. Osipov V.I., (1979). *Nature of strength and deformation properties of clay rocks*. Moscow, in Russian.
- 9 53. Osipov V.I., Sokolov V.N., Rumiantseva N.A., (1989). *Microstructure of clay rocks*. Moscow, Nedra. In  
10 Russian.
- 11 54. Peksa, A. E., Wolf, K. H. A. A., Slob, E. C., Chmura, L., & Zitha, P. L. J. (2017). Original and  
12 pyrometamorphical altered Bentheimer sandstone; petrophysical properties, surface and dielectric behavior.  
13 *Journal of Petroleum Science and Engineering*, 149, 270–280. <https://doi.org/10.1016/j.petrol.2016.10.024>
- 14 55. Plaza, R. C., González-Caballero, F., & Delgado, A. V. (2001). Electrical surface charge and potential of  
15 hematite/yttrium oxide core–shell nanoparticles. *Colloid and Polymer Science*, 279(12), 1206-1211.  
16 doi:10.1007/s003960100578
- 17 56. Pooryousefy, E., Xie, Q., Chen, Y., Sari, A., & Saeedi, A. (2018). Drivers of low salinity effect in sandstone  
18 reservoirs. *Journal of Molecular Liquids*, 250, 396-403. doi:<https://doi.org/10.1016/j.molliq.2017.11.170>
- 19 57. Priisholm, S., Nielson, B.L., Haslund, O. (1987). Fines migration, blocking, and clay swelling of potential  
20 geothermal sandstone reservoirs, Denmark. *SPE Formation Evaluation*, 168-178. Doi:10.2118/15199-PA
- 21 58. Raghavan, S. R.; Hou, J.; Baker, G. L.; Khan, S. A. (2000). Colloidal Interactions between Particles with  
22 Tethered Nonpolar Chains Dispersed in Polar Media: Direct Correlation between Dynamic Rheology and  
23 Interaction Parameters. *Langmuir*, 16, (3), 1066-1077.
- 24 59. Rohem Peçanha, E.; da Fonseca de Albuquerque, M. D.; Antoun Simão, R.; de Salles Leal Filho, L.; de  
25 Mello Monte, M. B. (2019). Interaction forces between colloidal starch and quartz and hematite particles in  
26 mineral flotation. *Colloids and Surfaces A: Physicochemical and Engineering Aspects*, 562, 79-85.
- 27 60. Rosenbrand, E., Kjøller, C., Riis, J. F., Kets, F., & Fabricius, I. L. (2015). Different effects of temperature  
28 and salinity on permeability reduction by fines migration in Berea sandstone. *Geothermics*, 53, 225-235.  
29 doi:<https://doi.org/10.1016/j.geothermics.2014.06.004>

- 1 61. Rostami, A., & Nasr-El-Din, H. (2010). A new technology for filter cake removal. *Society of Petroleum*  
2 *Engineers - SPE Russian Oil and Gas Technical Conference and Exhibition 2010, RO and G 10*, 2(October),  
3 1063–1079.
- 4 62. Russell, T., Chequer, L., Badalyan, A., Behr, A., Genolet, L., Kowollik, P., Bedrikovetsky, P. (2018).  
5 Systematic laboratory and modelling study of kaolinite in rocks on formation-damage-fines-migration non-  
6 equilibrium effects, analytical model. *Proceedings - SPE International Symposium on Formation Damage*  
7 *Control, 2018-Febru*. <https://doi.org/10.2118/189533-ms>
- 8 63. Russell, T., Chequer, L., Borazjani, S., You, Z., Zeinijahromi, A., & Bedrikovetsky, P. (2018). *Formation*  
9 *Damage by Fines Migration : Mathematical and Laboratory Modeling , Field Cases*. Elsevier, Amsterdam,  
10 69-175. <https://doi.org/10.1016/B978-0-12-813782-6.00003-8>
- 11 64. Sarkar, A. K., Sharma, M. M. (1990). Fines Migration in Two-Phase Flow. *Journal of Petroleum*  
12 *Technology*, (May), 646–652.
- 13 65. Schroth, B. K., & Sposito, G. (1997). Surface charge properties of kaolinite. *Clays and Clay Minerals*, 45(1),  
14 85–91.
- 15 66. Sharma M.M., Yortsos Y.C. (1987) Fines migration in porous media. *AIChE Journal*, 10 (33), 1654–1662.
- 16 67. Sheng, J. (2010). *Modern chemical enhanced oil recovery: Theory and practice*; Gulf: Burlington, MA,  
17 USA.
- 18 68. Skoglund, S.; Lowe, T. A.; Hedberg, J.; Blomberg, E.; Wallinder, I. O.; Wold, S.; Lundin, M. (2013). Effect  
19 of Laundry Surfactants on Surface Charge and Colloidal Stability of Silver Nanoparticles. *Langmuir*, 29,  
20 (28), 8882-8891.
- 21 Tadros, T.F. (2014). *General Principles of Colloid Stability and the Role of Surface Forces*. Wiley-VCH  
22 Verlag GmbH & Co. KGaA, 1-22.
- 23 69. Tchistiakov, A. A. (2000). Colloid chemistry of in-situ clay-induced formation damage. *SPE International*  
24 *Symposium on Formation Damage Control, Lafayette*, 371–379. <https://doi.org/10.2523/58747-ms>.
- 25 70. Tchistiakov, A. (2000). Physico-chemical aspects of clay migration and injectivity decrease of geothermal  
26 clastic reservoirs. *Proceedings World Geothermal Congress*, 3087-3095.
- 27 71. Tchistiakov., A. (2000). Physico-Chemical Factors Controlling In-Situ Clay-Induced Formation Damage  
28 During Water Re-Injection. *Proceedings of ETCE 2000 & OMAE 2000 Joint Conference Energy for the*  
29 *New Millennium*, February 14-17, New Orleans, USA.



- 1 72. Tchistiakov A. A., Sokolov V.N., Osipov V.I. (2001). Saponite clay tailing treatment by artificial  
2 sedimentation. *Clay Science for Engineering*, Adachi & Fukue (eds), Balkema, Rotterdam, ISBN  
3 9058091759.
- 4 73. Torkzaban, S., Bradford, S. A., & Walker, S. L. (2007). Resolving the Coupled Effects of Hydrodynamics  
5 and DLVO Forces on Colloid Attachment in Porous Media. *Langmuir*, 23(19), 9652-9660.  
6 doi:10.1021/la700995e
- 7 74. Vaidya, R. N., & Fogler, H. S. (1990). Formation damage due to colloiddally induced fines migration.  
8 *Colloids and Surfaces*, 50, 215-229. doi:https://doi.org/10.1016/0166-6622(90)80265-6
- 9 75. Vaidya, R. N., & Fogler, H. S. (1992). Fines migration and formation damage: Influence of pH and ion  
10 exchange. *Society of Petroleum Engineers - SPE Production Engineering 1992*, (November), 325-330.
- 11 76. Wijenayaka, L. A., Ivanov, M. R., Cheatum, C. M., Haes, A. J. (2015). Improved Parametrization for  
12 Extended Derjaguin, Landau, Verwey, and Overbeek Predictions of Functionalized Gold Nanosphere  
13 Stability. *The Journal of Physical Chemistry C*, 119(18), 10064-10075.
- 14 77. Xu, C.-y., Deng, K.-y., Li, J.-y., Xu, R.-k. (2015). Impact of environmental conditions on aggregation  
15 kinetics of hematite and goethite nanoparticles. *Journal of Nanoparticle Research*, 17(10), 394.
- 16 78. You, Z., Aji, K., Badalyan, A., & Bedrikovetsky, P. (2012). Effect of nanoparticle transport and retention in  
17 oilfield rocks on the efficiency of different nanotechnologies in oil industry. *Society of Petroleum Engineers*  
18 - *SPE International Oilfield Nanotechnology Conference 2012*, (June), 397-411.  
19 <https://doi.org/10.2118/157097-ms>
- 20
- 21

## 1. Figures and Tables

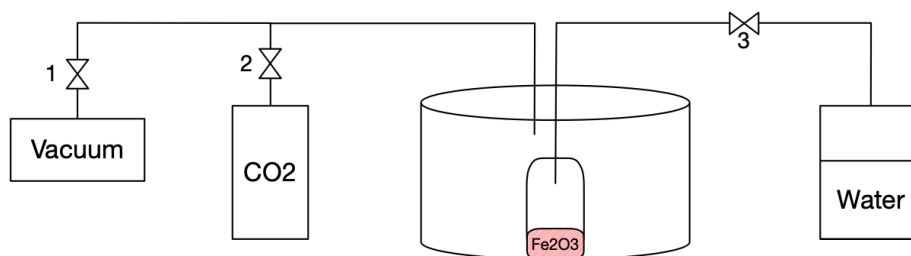


Figure 1 – Setup for preparation of hematite suspension. The hematite powder was vacuumed through valve 1 and CO<sub>2</sub> and water were further added through valves 2 and 3 respectively.

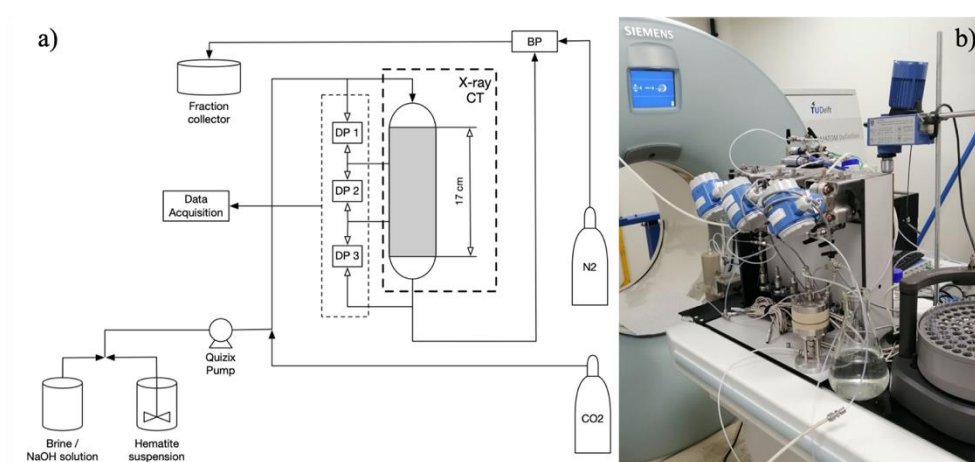


Figure 2 – a) The schematic drawing of the experimental setup used to perform the core-flood experiments.

DP = differential pressure, BP = back pressure; b) photo of the setup.

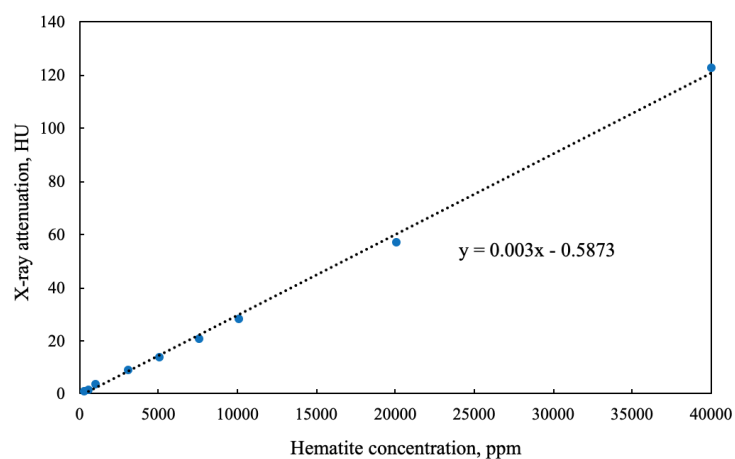
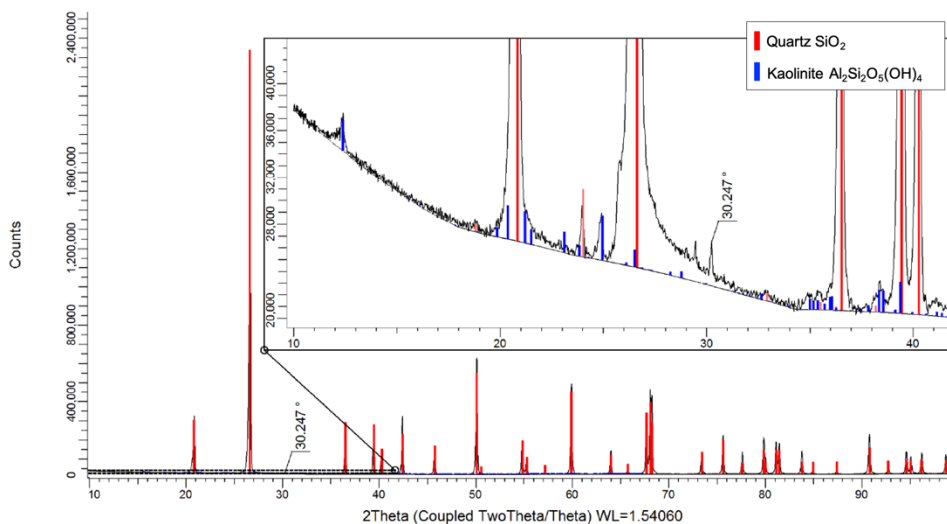
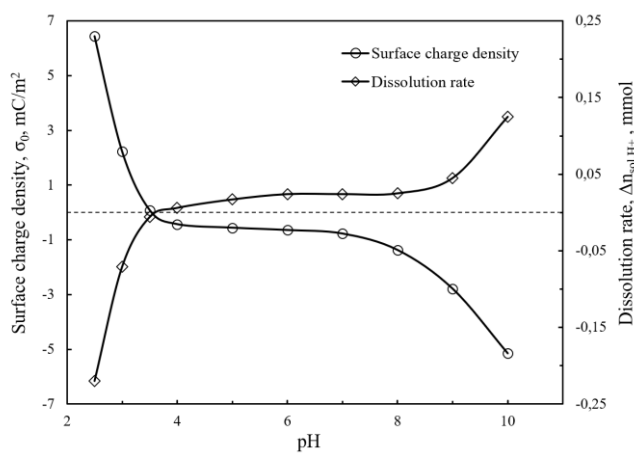


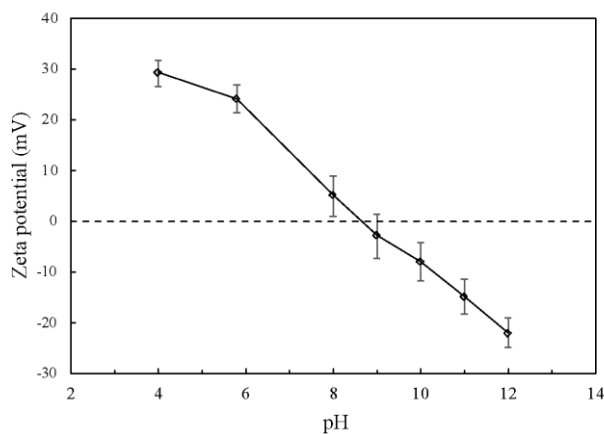
Figure 3 – Calibration curve of CT value as a function of hematite concentration. The concentration ranging from 0 to 40,000 was used. The dashed line represents the linear trend line of the concentration.



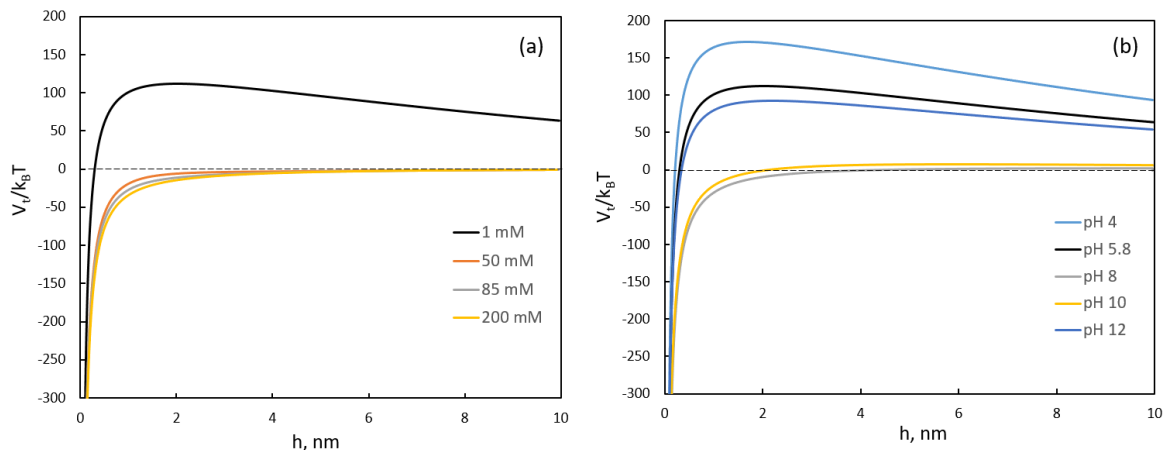
1  
2 Figure 4 – XRD pattern of the pulverized Bentheimer sample used for Exp.1 1. Based on the semi-  
3 quantitative approach, silica was found to be the main compound in the rock ( $99.3 \pm 0.1$  wt%). There was also a  
4 small fraction of kaolinite ( $0.7 \pm 0.1$  wt%)



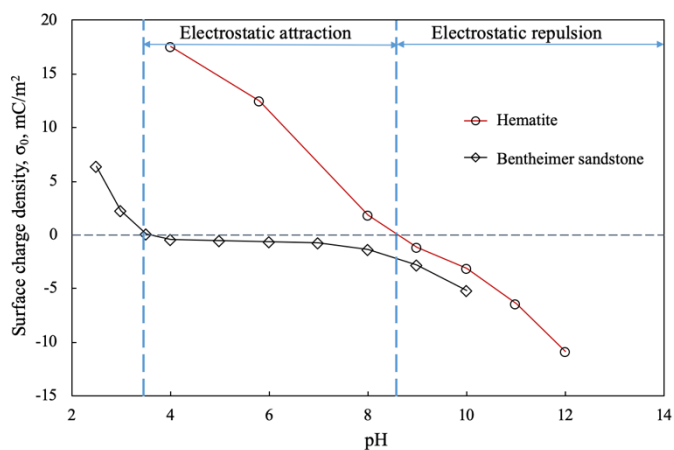
5  
6 Figure 5 – Estimation of the dissolution rate and surface charge density as a function of pH for the  
7 Bentheimer sample used in the core-flood experiments based on the potentiometric mass titration data. Above  
8 the PZC= $3.4 \pm 0.1$ , the rock surface is negatively charged



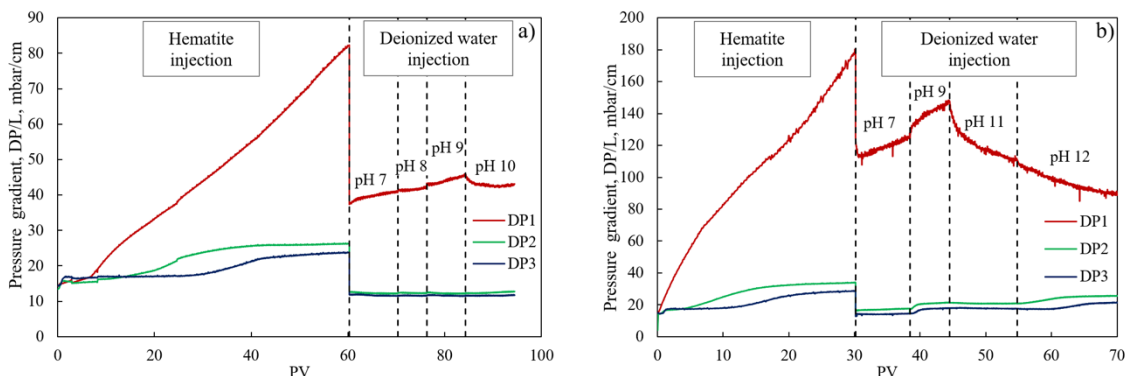
9  
10 Figure 6 – Zeta potential measurements at various pH to identify the PZC of hematite particles. The PZC  
11 was found at  $\text{pH } 8.5 \pm 0.1$



1  
2 Figure 7 – Inter-particle interaction potential ( $V_i$ ) as a function of particle separation distance ( $h$ ) calculated  
3 by DLVO theory: a) Effect of ionic strength on hematite particle interaction at pH 5.8; b) Effect of pH on  
4 hematite particle interaction at  $I=1$  mM using zeta potential values given in Figure 6



5  
6 Figure 8 – The estimated surface charge density for the hematite particles and the Bentheimer sample used  
7 in the core-flood experiments. In the pH ranging from  $3.4 \pm 0.1$  to  $8.5 \pm 0.1$ , the interaction between the  
8 particles and rock surface is dominated by the electrostatic attraction whereas at  $pH > 8.5 \pm 0.1$  is dominated by  
9 electrostatic repulsion.



10  
11 Figure 9 – Pressure gradient as the function of PV injected during core-flood experiments in three sections  
12 of the core: a) Exp. 1, injection of hematite suspension and deionized water with pH 7-10, b) Exp. 2 injection of  
13 hematite suspension and deionized water with pH 7-12  
14

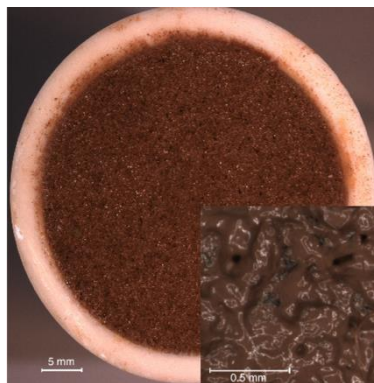


Figure 10 – Filter cake observed at the core inlet as a result of injection of hematite suspension (Exp. 1)

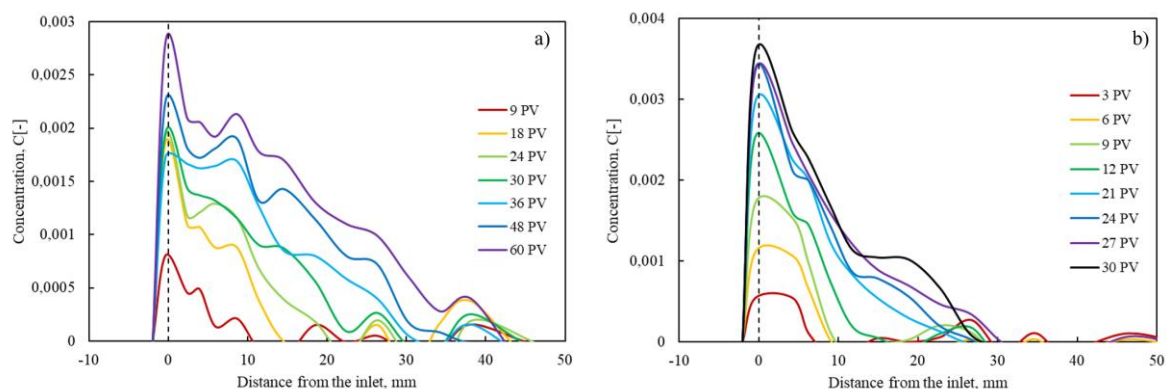


Figure 11 – Hematite concentration as a function of distance from core inlet: a) Exp. 1, from 9 PV to 60 PV, b) Exp. 2, from 3 PV to 30 PV. All the data shown correspond to section 1 of the cores.

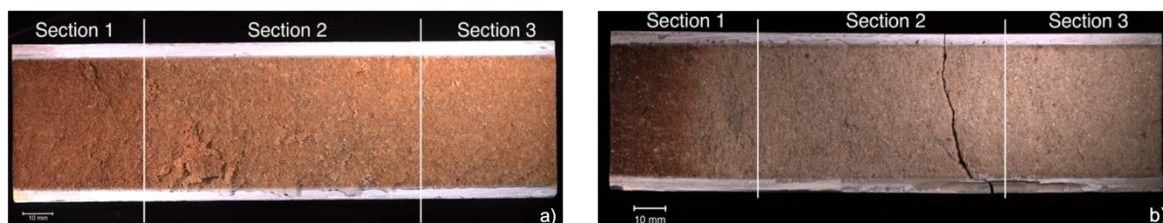


Figure 12 –Microscopic image of the core after core-flood experiments: a) Exp. 1, b) Exp. 2.

1

Table 1 – Properties of Bentheimer core samples

|                      |                |               |
|----------------------|----------------|---------------|
| Components           | Quartz         | Kaolinite     |
|                      | 99.3 ± 0.1 wt% | 0.7 ± 0.1 wt% |
| Porosity             | 24.4 ± 0.2 %   |               |
| Initial Permeability | Exp. 1         | Exp. 2        |
|                      | 1770 ± 20 mD   | 1400 ± 20 mD  |

2

Darcy (D) - permeability of the porous medium through which the flow of 1cm<sup>3</sup> of fluid with viscosity of 1 cp in 1 sec under the differential pressure of 1 atm, where the porous medium has cross-sectional area of 1 cm<sup>2</sup> and

4

length of 1 cm. 1 mD ≈ 1 μm<sup>2</sup>·10<sup>-3</sup>.

1  
2

Table 2 – Parameters of the experiments

|        | Permeability | Stage 1             | Stage 2         | Stage 3       | Stage 4       | Stage 5       |
|--------|--------------|---------------------|-----------------|---------------|---------------|---------------|
| Exp. 1 | 1770 ± 20 mD | Hematite suspension | Deionized water |               |               |               |
|        |              |                     | pH 7            | pH 8          | pH 9          | pH 10         |
|        |              | Q = 25 mL/min       | Q = 10 mL/min   | Q = 10 mL/min | Q = 10 mL/min | Q = 10 mL/min |
|        |              | V = 60 PV           | V = 10 PV       | V = 6 PV      | V = 8 PV      | V = 10 PV     |
| Exp. 2 | 1400 ± 20 mD | Hematite suspension | Deionized water |               |               |               |
|        |              |                     | pH 7            | pH 9          | pH 11         | pH 12         |
|        |              | Q = 25 mL/min       | Q = 10 mL/min   | Q = 10 mL/min | Q = 10 mL/min | Q = 10 mL/min |
|        |              | V = 30 PV           | V = 8 PV        | V = 6 PV      | V = 10 PV     | V = 20 PV     |

3  
4

Table 3 – Permeability of the core sample before and after Exp. 1

|           | Permeability before,<br>mD ( $\mu\text{m}^2 \cdot 10^3$ ) | Permeability after, mD<br>mD ( $\mu\text{m}^2 \cdot 10^3$ ) | Permeability impairment |
|-----------|---|---|-------------------------|
| Total     | 1770  | 590   | 67 %                    |
| Section 1 | 1760  | 270   | 85 %                    |
| Section 2 | 1780  | 1010  | 43 %                    |
| Section 3 | 1760  | 950   | 46 %                    |

5  
6

Table 4 – Permeability of the core sample before and after Exp. 2

|           | Permeability before,<br>mD ( $\mu\text{m}^2 \cdot 10^3$ ) | Permeability after,<br>mD ( $\mu\text{m}^2 \cdot 10^3$ ) | Permeability impairment |
|-----------|---|--|-------------------------|
| Total     | 1460  | 240  | 84 %                    |
| Section 1 | 1470  | 90   | 94 %                    |
| Section 2 | 1460  | 500  | 66 %                    |
| Section 3 | 1450  | 430  | 70 %                    |

7

**Credit Author Statement**

| Name                  | Contribution   |
|-----------------------|--|
| Anna K. Kottsova      | Conceptualization, methodology, validation, formal analysis, investigation, resources, writing - original draft, writing - review & editing. |
| Mohsen Mirzaie Yegane | Supervision, methodology, investigation, resources, writing - review & editing   |
| Alexei A. Tchistiakov | Conceptualization, methodology, validation, writing - review & editing, supervision  |
| Pacelli L.J. Zitha    | Conceptualization, methodology, validation, resources, writing - review & editing, supervision   |



Skolkovo Institute of Science and Technology

Anna Kottsova

PhD student

Skolkovo Institute of Science and Technology

Center for Hydrocarbon Recovery

Dear Sir / Madam,

We submit for your consideration the revised manuscript COLSUA-D-20-02419R1 entitled “Effect of electrostatic interaction on the retention and remobilization of colloidal particles in porous media” by Anna K. Kottsova, Mohsen Mirzaie Yegane, Alexei A. Tchistiakov and Pacelli L.J. Zitha.

On behalf of all authors, I declare that I have disclosed all competing interests related to this work. If any exist, they have been included in the “Declaration of Interests” section of the manuscript.

Sincerely,

A handwritten signature in black ink, appearing to read "Anna Kottsova".

Anna Kottsova



# Effect of electrostatic interaction on the retention and remobilization of colloidal particles in porous media

Anna K. Kottsova<sup>a,\*</sup>, Mohsen Mirzaie Yegane<sup>b</sup>,  
Alexei A. Tchistiakov<sup>a</sup>, Pacelli L.J. Zitha<sup>b</sup>

<sup>a</sup> Skoltech Center for Hydrocarbon Recovery, Skolkovo Institute of Science and Technology, Bolshoy Boulevard 30, bld. 1, Moscow, 121205, Russia

<sup>b</sup> Department of Geoscience and Engineering, Delft University of Technology, Stevinweg 1, Delft, 2628 CN, the Netherlands

\*Corresponding author. E-mail address: Anna.Kottsova@skoltech.ru

Keywords: fines, hematite particles, point of zero charge, van der Waals, electrostatic, interactions

## Abstract

We investigate the effect of pH on external hematite colloidal particles entrapment and remobilization by core-flood experiments combined with X ray computed tomography. Suspensions of calibrated hematite colloidal particles were injected into Bentheimer sandstones sample, composed mainly of well-sorted quartz and small clay fraction (up to 1 wt%), consisting mainly of kaolinite. We have found that permeability impairment due to an external cake build-up can be reversed when pH exceeds the point of zero charge of hematite particles. This effect could be successfully interpreted by the switching of the surface charge of hematite particles from positive to the negative, similar to the rock surface. The experimentally verified pH-controlled electrostatic retention and remobilization technique can be extended to other colloidal particles, having pH-dependent surface charge, including natural clay minerals in hydrocarbon and geothermal reservoirs. Therefore, varying pH of injected fluid can be applied for targeted external cake build-up and transportation of colloidal particles within a reservoir.

## 1. Introduction

Colloidal fines migration is a common phenomenon in various industrial processes relying on fluid flow in porous media, including hydrology (McDowell-Boyer et al., 1986; Torkzaban et al., 2007), geothermal engineering (Mahmoudi et al., 2010; Rosenbrand et al., 2015), gas production from hydrate-bearing sediments (Jung et al., 2012), well-bore drilling (Byrne et al., 2007; Civan, 2007), and enhanced oil recovery (EOR), where low salinity water injection emerged as a new approach to mobilize additional oil (Alshakhs & Kovsky, 2016; Iglauer et al., 2010; Nasralla et al., 2013; Pooryousefy et al., 2018; Xie et al., 2016). Water injection applied within these processes can cause impairment of permeability due to blockage of pores at the borehole walls by

1  
2  
3  
4  
5  
6  
7 1 particles, suspended in the water, or due to entrapment of migrating in-situ clay particles in pore throats within  
8  
9 2 the reservoir.

10 3 Fines migration in porous media has been intensively investigated in the last few decades (Lei et al., 2017;  
11  
12 4 Yu et al., 2019). It was established that attachment or detachment of colloidal particles from pore walls and  
13  
14 5 following up their migration in porous media are determined by the balance of forces acting between the particles  
15  
16 6 and the rock mineral grains surfaces. The attachment occurs thanks to London – van der Waals attraction forces.  
17  
18 7 The detachment can be triggered by combined effect of repulsive forces such as the electrostatic repulsion of  
19  
20 8 overlapping electrical double layers (EDL), if the surface charge of clay particles and the rock matrix has the same  
21  
22 9 sign, structural forces of bound water, hydrodynamic drive of flowing fluid. (Vaidya & Fogler, 1990; Elimelech  
23  
24 10 (1991, 1995); Tchistiakov, 2000; Kalantariasl & Bedrikovetsky, 2014, Kobayashi, 2005).

25  
26 11 The electrostatic repulsion considerably depends on the fluid salinity as the latter changes  $\zeta$ -potentials of the  
27  
28 12 interacting surfaces. The repulsion between a clay particle and a pore wall decreases with the rise of ionic strength  
29  
30 13 of the pore aqueous solution and increases when the fluid salinity drops. It was experimentally demonstrated, that  
31  
32 14 at low salinity of the injected fluid in-situ particles could be detached from the rock matrix surface and deposited  
33  
34 15 downstream that led to significant reduction of the rock permeability (Kia et al., 1987; Vaidya & Fogler, 1990;  
35  
36 16 Tchistiakov, 2000; Rosenbrand et al., 2015; Alshakhs, & Kovscek, 2016; A. Al-Sarihi et al., 2018; Borazjani et  
37  
38 17 al., 2018:).

39  
40 18 Besides salinity, the electrostatic interaction between clay particles and the rock mineral matrix is controlled  
41  
42 19 by the pore fluid pH (Kia et al., 1987; Vaidya & Fogler, 1990, 1992; ; Mietta et al., 2009; Kobayashi et al., 2009;  
43  
44 20 You et al., 2012; Kumar et al., 2017 ). It was experimentally confirmed that an increase of pH above a certain  
45  
46 21 critical value causes charge reversal of natural clay  $\zeta$ -potential from positive to negative. The critical pH value,  
47  
48 22 when  $\zeta$ -potential becomes zero, is called point of zero charge (Olphen H. van, 1963; Osipov V. I, 1979; Mitchell,  
49  
50 23 1993). For clay particles, the point of zero charge (PZC) can vary significantly depending on their mineralogy and  
51  
52 24 crystal structure, however at pH values feasible for sandstone formations it is always larger than the point of zero  
53  
54 25 charge of quartz that is commonly a predominant component of the sandstones matrix (Churcher et al., 2015;  
55  
56 26 Didier et al., 2015; Kosmulski, 2016; Schroth, 1997, Osipov 1979). This means that at certain pH values, in-situ  
57  
58 27 clay particles as well as external colloidal particles, present in the fluid injected in the formation, can have a  
59  
60 28 surface charge of the same or opposite sign with the charge of the rock pore surface. This means that we can  
61  
62 29 theoretically manage migration and retention of in-situ and external colloidal particles within a reservoir porous  
63  
64 30 medium by varying pH. Some research on this subject has already been done. For example Kumar et al. (2017)  
65

1  
2  
3  
4  
5  
6  
7 1 has experimentally shown that an increase of pH causes increase of the magnitude of the long-range repulsion  
8 2 between a SiO<sub>2</sub> tip and a silica facet of kaolinite. The experiments were done within the range of pH above  
9 3 kaolinite's PZC and thus no charge reversal occurred. Kobayashi et al. (2009) have investigated the effect of pH  
10 4 alteration on retention of latex particles by a zirconia bed and concluded that pH increase had minor effect on the  
11 5 retention in comparison with salinity rise.

12 6 Although considerable efforts have been made to investigate the effect of pH variation on external particle  
13 7 migration and retention by different materials today we still do not have confident and experimentally confirmed  
14 8 methodology of these process management in natural reservoirs.

15 9 The main objective of this research was to examine the possibility of artificial management of external  
16 10 colloidal particles retention by natural sandstone matrix and remobilization by gradual increase of pH of the  
17 11 injected fluid above the mineral point of zero charge. In previous studies pressure and effluent data were mainly  
18 12 used for monitoring fines migration within rock porous media, in the present study next to differential pressure  
19 13 measurements we applied X-ray tomography for tracking the migration of remobilized particles. Hematite  
20 14 particles were chosen as model particles because of their pH-dependent surface charge, distinguishable red color,  
21 15 and high density and X-ray attenuation capacity, which make them detectable for CT-assisted core-flood  
22 16 experiments. Bentheimer sandstone was used as the model porous medium. Prior to core-flood experiments,  
23 17 characterization of the rock and particles properties was performed and colloidal stability of the hematite  
24 18 suspension at various ionic strength and pH was studied by the DLVO theory. For core-flood experiments, a  
25 19 suspension of hematite particles was injected to deposit the particles within the porous media. Thereafter,  
26 20 deionized water with gradually increasing pH above the PZC of hematite particles was injected to give rise to a  
27 21 repulsion term between particles and sandstone surface and consequently to remobilize the deposited particles.  
28 22 We establish theoretical and experimental conclusions that presumably can be extended to other minerals with  
29 23 pH-dependent surface charge, including natural minerals in porous media.

30 24 The paper proceeds with description of materials and methods used for the experiments, where both  
31 25 preparation steps and experimental methodology are illustrated. Then, the experimental results are shown,  
32 26 followed by the general discussion and conclusions.

## 33 27 **2. Materials and methods**

### 34 28 *2.1 Porous medium*

35 29 The core-flood experiments were performed with Bentheimer sandstone of Early Cretaceous age from the  
36 30 south-western part of the Lower Saxony Basin. Bentheimer sandstone outcrop samples are often used as model  
37  
38  
39  
40  
41  
42  
43  
44  
45  
46  
47  
48  
49  
50  
51  
52  
53  
54  
55  
56  
57  
58  
59  
60  
61  
62  
63  
64  
65

1  
2  
3  
4  
5  
6  
7 1 natural porous medium for laboratory studies because of their lateral continuity and block scale homogeneous  
8  
9 2 nature (Peksa et al., 2017). The high permeability and large pore size of Bentheimer samples make it an appealing  
10 3 candidate to study the migration of colloidal particles in porous media and the ensuing permeability reduction.  
11  
12 4 Bentheimer sandstone, consists of more than 85% of pore throats have a size larger than 10  $\mu\text{m}$  and only 5% of  
13 5 them are smaller than 5  $\mu\text{m}$  (Peksa et al., 2015). Table 1 shows the physical properties of Bentheimer core samples  
14 6 used to conduct the core-flood experiments. After cutting and drying the cores in an oven for up to 48 hours at 60  
15 7  $\pm 1$   $^{\circ}\text{C}$ , the cores were placed in molds and encased in an epoxy resin to prevent bypassing the flow alongside the  
16 8 core. The penetration depth of the resin into the core was nearly 1.0 mm. Thereafter, the cores were precisely  
17 9 machined to an effective diameter of  $3.8 \pm 0.1$  cm and a length of  $17.0 \pm 0.1$  cm. The machined samples were  
18 10 dried for 15 hours in an oven at  $40 \pm 1$   $^{\circ}\text{C}$ . The porosities of the core samples were measured by the Helium gas  
19 11 expansion method. The permeability of the cores was estimated using Darcy's law, by flowing 5000 ppm NaCl  
20 12 brine at different rates within the core and recording the pressure drop. It should be noted that the characterization  
21 13 of the rock with XRD analysis and potentiometric titration measurements were performed on the rock sample  
22 14 pulverized to 1  $\mu\text{m}$  powder.

## 28 15 2.2 Chemicals

30 16 Hematite ( $\alpha\text{-Fe}_2\text{O}_3$  with density equal to 5.24  $\text{g}/\text{cm}^3$ ) particles were supplied by Sigma-Aldrich in powder  
31 17 form with. The high density of the particles results in high attenuation of X-rays relative to quartz, the main  
32 18 component of the sandstone. The diameter of an individual particle was  $< 50$  nm, as reported by the manufacturer,  
33 19 which was obtained from BET; however, they had a strong tendency to aggregate and form larger particles,  
34 20 therefore in this study we further refer to them as colloidal particles. Moreover, as mentioned, hematite particles  
35 21 had a distinguishable red color that simplified their detection in effluent and during the microscopic examination  
36 22 of the sample slab after core-flood experiments. Sodium chloride (NaCl) used for brine preparation was purchased  
37 23 from Sigma-Aldrich as well. The base (1 M NaOH) and acid (1 M HCl) used for pH adjustment, were supplied  
38 24 by Merck KGaA.

44 25 Aqueous suspensions of hematite were used to deposit particles inside the rock porous media. Earlier studies  
45 26 have shown that aggregation of hematite particles increases drastically with the addition of a small quantity of  
46 27 salt into the aqueous solution (Dickson et al., 2012; He et al., 2008). This is supported by our analysis of the  
47 28 colloidal stability of hematite suspensions. Therefore, in these experiments, we use hematite suspension in  
48 29 ultrapure [deionized water \(DI water\)](#). As for initial saturation of the core, 5000 ppm NaCl brine was used to  
49 30 prevent clogging of pores with released in-situ clay particles before the beginning of the experiment.

### 2.3 Preparation of hematite suspension

In order to avoid air entrapment inside of the hematite aggregates and produce an air-free stable suspension of hematite particles, the following preparation procedure was applied. First, the particles were placed into a vacuum, then saturated with CO<sub>2</sub> and after secondary vacuuming mixed with [deionized water](#) and stirred (Figure 1). This was followed by sonication at the power of 550W, 20 kHz, and an amplitude of 20%. The applied procedure allowed preparing a colloidally stable suspension with no observable sedimentation. The pH of the prepared suspension was measured to be  $5.8 \pm 0.1$ . Hematite suspension of 250 ppm concentration prepared in [deionized water](#) was applied in flooding tests. During the core-flood experiments, the suspension in the tank was continuously stirred in order to maintain its homogeneity.

### 2.4 Characterization of rock and hematite particles

#### 2.4.1 XRD analysis

XRD analysis was performed to determine the composition of the rock. The XRD data were obtained on a Bruker D8 Advance diffractometer equipped with a Bragg-Brentano geometry and Lynxeye position sensitive detector and using Cu K $\alpha$  radiation. The pulverized rock was placed into an appropriate holder and its surface was made as flat as possible prior to the analysis. The scans were done with rotation on, at 45 kV and 40 mA. The measurement was performed with a coupled  $\theta$  - $2\theta$  scan with a step size of 0.025° and time per step of 2 seconds. The Semi-quantitative (S-Q) approach was used to approximate the fractions of the identified phases. The fractions were calculated with Bruker Diffrac.Eva software using the height of the peaks after ka2 stripping and the ratio  $I/I_{cor}$  from the ICDD PDF-4+ 2020 database.

#### 2.4.2 Potentiometric mass titration

The potentiometric mass titration (PMT) method was used to identify the point of zero charge (PZC) of the rock. 100 mL of 1,500 ppm NaCl (~ 0.025 mM) solution, as the background solution, was put into three different flasks. The pulverized rock with different masses of 2.5, 5.0, and 10.0 g was transferred to each flask. A blank solution without the addition of rock powder was also prepared. Before the experiment, the suspensions were stirred with a Teflon magnetic stirrer for 24 h to reach an equilibrium. Then potentiometric titrations were performed in a nitrogen atmosphere. First, 5 mL of 0.1 M NaOH was added to all flasks to deprotonate a significant portion of the surface sites, causing the surface to be negative. Next, each of these suspensions and the blank sample were titrated by addition of 0.1 M HCl to the cell in 10 – 15 steps. The samples were continuously stirred, except when the pH was recorded after every 2 – 5 min while the stirrer was switched off.

The pH-dependent surface charge density ( $\sigma_0$ ) was determined based on the measured PMT data, according to the following equation (Lützenkirchen et al., 2012):

$$\sigma_0(pH) = \frac{F \cdot (\Delta n_{sol,H^+}(pH) - \Delta n_0)}{m S_{BET}} \quad (1)$$

where  $F$  is the Faraday constant ( $F = 96500$  C/mol),  $m$  is the mass of the sample,  $S_{BET}$  is the rock specific surface area and  $\Delta n_0$  is the pH-dependent amount of acid which is consumed on a sample with a very small mass (extrapolated to zero mass). The dissolution effect ( $\Delta n_{sol,H^+}$ ) is obtained by comparison of the balance of protons ions in the potentiometric titration of suspensions with the blank potentiometric titration results according to the following equation:

$$\Delta n_{sol,H^+} = \Delta n_{acid(s)}(pH) - \Delta n_{acid(B)}(pH) \quad (2)$$

where  $\Delta n_{acid(s)}(pH)$  and  $\Delta n_{acid(B)}(pH)$  represent the balance of protons ions needed to be consumed to reach a certain pH for the suspension and blank respectively.

#### 2.4.3 Zeta potential and particle size distribution

The zeta potential and hematite particles size distribution (PSD) in [deionized water](#) were measured using a Malvern Zetasizer Nano ZS at 25 °C. [Zeta potential is calculated by means of Henry's equation from the measured electrophoretic mobility](#). In order to enable measurements on this instrument the particles concentration was adjusted to provide a count rate of ca. 500 kcps. Samples were run in triplicate in the auto mode and the average was recorded. There was a pause of 30 – 60 sec between each run, for relaxation of the sample.

#### 2.5 Hematite inter-particle interactions

Dispersed particles are subject to Brownian motion which causes frequent inter-particle collisions. The balance between inter-particle interactions determines whether the dispersion of hematite particles is colloiddally stable. According to the DLVO theory (Hotze et al., 2012; Mirzaie Yegane et al., 2020; Skoglund et al., 2013), the total energy for the interaction between two unmodified spherical particles ( $V_t$ ) with radius  $R$ , at separation distance  $h$  is given by the sum of van der Waals ( $V_v$ ) and electrostatic ( $V_e$ ) potentials:

$$V_t(x) = V_v(x) + V_e(x) \quad (3)$$

where  $x$  is the normalized separation distance equal to  $h/R$ . The van der Waals potential is (Israelachvili, 2011):

$$\frac{V_v(x)}{k_B T} = -\frac{(\sqrt{A_H} - \sqrt{A_W})^2}{6k_B T} \left\{ \frac{2}{x(x+4)} + \frac{2}{(x+2)^2} + \ln \left[ \frac{x(x+4)}{(x+2)^2} \right] \right\} \quad (4)$$

where  $A_H$  and  $A_W$  are Hamaker constants for hematite particle and water, as the medium, respectively (Raghavan et al., 2000),  $k_B$  is the Boltzmann's constant and  $T$  is the absolute temperature. The electrostatic potential is described (Oshima, 1995) by:

$$\frac{V_e(x)}{k_B T} = \frac{2\pi\epsilon_0\epsilon_r\psi_0^2 R}{k_B T} \ln[1 + \exp(-\kappa R x)] \quad (5)$$

where  $\epsilon_0$  is the vacuum permittivity,  $\epsilon_r$  is the medium relative permittivity,  $\psi_0$  is the surface potential and  $\kappa^{-1}$  is Debye length which is given by:

$$\kappa^{-1} = \left( \frac{\epsilon_0\epsilon_r k_B T}{2N_A e^2 I} \right)^{0.5} \quad (6)$$

where  $e$  is the electronic charge,  $N_A$  is the Avogadro's number, and  $I$  is the medium ionic strength (Tadros, 2014).

Surface potential is estimated based on the zeta potential ( $\zeta$ ) using Equation 7. [The Equation is obtained by solving the Poisson-Boltzmann equation for a distribution of the point charges that decay as a function of the radial distance from the surface of charged particle \(Wijenayaka et al., 2015\):](#)

$$\psi_0 = \zeta \left( 1 + \frac{1}{\kappa R} \right) \exp(1) \quad (7)$$

The pH-dependent surface charge density ( $\sigma_0$ ) can be calculated according to Equations 8-9 (Plaza et al., 2001):

$$\sigma_0 = \frac{2\epsilon_0\epsilon_r\kappa k_B T}{e} \sin h \left( \frac{e\psi_0}{2k_B T} \right) \times \left[ 1 + \frac{1}{\kappa R} F(T) + \frac{1}{(\kappa R)^2} G(T) \right]^{1/2} \quad (8)$$

$$F(T) = \frac{2}{\cos h^2 \left( \frac{e\psi_0}{4k_B T} \right)}; \quad G(T) = \frac{8 \ln \left[ \cos h \left( \frac{e\psi_0}{4k_B T} \right) \right]}{\left( \frac{e\psi_0}{2k_B T} \right)} \quad (9)$$

Dispersions of particles stay kinetically stable if the potential barrier ( $V_{max}$ ) is larger than  $\sim 16/k_B T$  (Berg, 2010; Mirzae Yegane et al., 2020; Moskovits et al., 2005).

It should be noted that the terms point of zero charge and isoelectric point are often used interchangeably, isoelectric point corresponds to the results obtained by the electrokinetic method, while the point of zero charge value is obtained by titration (Kosmulski et al., 2016). Plaza et al. (2010). observed that for hematite particles, the pH ( $\zeta = 0$ ) and pH ( $\psi_0 = 0$ ) are almost identical. Alvarez-Silva et al. (2010) also noted that PZC and IEP can be considered equal if no other specific adsorption of potential-determining ions happens. To avoid confusion between the surface potential of rock matrix surface and hematite particles, throughout this study we refer to this as the point of zero charge which is where the surface charge density is zero.

## 2.6 Core-flood experimental setup

The core-flood experiment setup is shown in Figure 2. The setup was placed on the couch of the CT scanner to enable monitoring of external particles migration during the core-flood experiments. A core sample was placed into a poly-ether-ether-ketone core holder, which is transparent to X-rays, and positioned in the gantry of the scanner. The core holder is oriented vertically in order to mitigate the effect of gravity on particles distribution within the injected fluid stream as well as within the core. The core holder had three differential pressure transducers (KEMA03 ATEX 1561) with  $\pm 300$  mbar range and  $\pm 1$  mbar accuracy to monitor pressure drop along the core during the experiment. Differential pressure was measured during core-flood experiments at the inlet, middle and outlet sections of the sample with lengths  $4.1 \pm 0.1$  cm,  $8.8 \pm 0.1$  cm, and  $4.0 \pm 0.1$  cm accordingly. Pressure drop over the core was also monitored using inlet and outlet pressure transducers, while the outlet pressure was set using a backpressure regulator (BPR). Fluids were injected into the core using a Quizix pump, which was operated at a constant flow rate. A fraction collector (GE Frac 920) was used for sampling the effluents at the core-holder outlet for visual detection and physical-chemical analysis of hematite particles at the outlet.

### 2.7 Core-flood experimental procedure

A set of core-flood experiments was performed for this study. For the discussion in the current paper we present the results of the two most representative experiments, further referred to as Experiment 1 and Experiment 2. The same experimental procedure was applied to all tests. During Exp. 1, we investigated the effect of a gradual rise in pH from neutral up to pH 10 and during Exp. 2 a steeper rise from neutral to pH 12 was studied in order to investigate the effect of pH values further from PZC of hematite on the remobilization of the particles.

The tests were performed in three stages. First, the core sample was saturated with 5000 ppm NaCl brine and its permeability to brine was determined using Darcy's law (Darcy, 1856). Then hematite suspension in [deionized water](#) was injected at sufficiently high flow rate (25 mL/min) to prevent the gravitational segregation of the particles (Dickson et al., 2012; He et al., 2008). 60 pore volumes (PV) of hematite suspension were injected in Experiment 1, and 30 PV in Experiment 2. Lower volume injected in Exp. 2 was dictated by the significantly higher differential pressure observed during the experiment because of lower permeability of the core (as will be discussed in more detail in Section 3.4)

Finally, the core was subjected to the injection of [deionized water](#) at gradually increasing pH. In Exp. 1, pH steps were 7, 8, 9, 10, in the second one 7, 9, 11, and 12. The [deionized water](#) injection rate in both tests was 10 mL/min. The other experimental parameters are summarized in Table 2. Before the core-flood experiments, the [deionized water](#) was passed through 0.5  $\mu\text{m}$  filter in order to prevent the effect of any solid impurities.



## 2.8 X-ray CT scanning

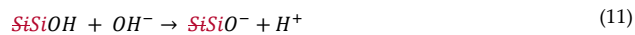
X-ray CT scanning was performed throughout the injection of both hematite suspension and [deionized water](#) in order to build hematite distribution profiles and track the movement of particles. Siemens SOMATOM Definition Dual Energy CT scanner with slice number of 64 slices per second and a resolution of 0.25 mm is used in this study. The scanning was performed at 140 KeV and 250 mA. To enable a quantitative analysis of hematite distribution along the core during core-flood experiments, we first established the calibration curve for CT scan number against hematite concentration by measuring the measured CT attenuation value (CT number) for hematite suspensions for solid phase concentrations ranging from 0 to 40,000 ppm. The resulting curve shown in Figure 3 show that the CT attenuation varies linearly with hematite concentration.

## 3. Results and discussion

### 3.1 Sandstone characterization

The characteristics of Bentheimer sandstone were extensively discussed in the literature (Al-Yaseri et al., 2015; Dubelaar et al., 2015; Peksa et al. 2015, 2017). Here, we only highlight the important aspects which are relevant to our study. As can be seen in Figure 4, the XRD analysis on the pulverized Bentheimer sample which was used for core-flood experiments shows, that it consists dominantly of quartz with very small fractions of kaolinite ( $99.3 \pm 0.1\text{wt}\%$  and  $0.7 \pm 0.1 \text{ wt}\%$  respectively). This is in very good agreement with observations of Farooq et al. (2011) and Al-Yaseri et al. (2015) who found that the fraction of quartz in Bentheimer sandstone is approximately 98 and 99 wt% respectively with a small fraction of kaolinite (0.5 and 0.7 wt% respectively). It should be noted that in our XRD analysis, a few very small peaks were not identified. Thus, there might be some phases present, which are not included in the fraction calculation.

The dielectric behavior of the Bentheimer sample was assessed based on the alteration in surface charge as a result of the change in the pH. The surface charge of silica, as the main component of the Bentheimer sandstone, is due to adsorption or dissociation of protons on the surface and the consequent ionization of the silanol groups represented by the following reactions (Davis et al., 1978; Lecourtier et al., 1990):



Based on the PMT method, the point of zero charge (PZC) of the Bentheimer sample was found to be  $3.4 \pm 0.1$  (see Figure S1 in the supplementary materials). This is in agreement with the finding of Farooq et al. (2011) who also used the PMT method and whose Bentheimer sample had a quartz fraction of approximately 98 wt%.

1  
2  
3  
4  
5  
6  
7 1 However, the value of PZC measured in this study differs from the observation of Peksa et al. (2015) whose  
8 2 Bentheimer sample had a quartz fraction of approximately 92 wt% and measured a PZC of nearly 8. They  
9 3 attributed this unexpected high PZC to the presence of clay (~ 2.7 wt%) and iron particles (0.2 wt%) distributed  
10 4 in the sample. Further work on this matter is not within the scope of this study. Figure 5 indicates the surface  
11 5 charge density and proton balance related to the dissolution effects based on the PMT data. Above the PZC, the  
12 6 sandstone surface was dominated by SiO<sup>-</sup> sites and as a result, it became negatively charged. The magnitude of  
13 7 negative surface charge density increases with increasing pH due to the dissociation of silanol groups. Such an  
14 8 increase is more pronounced at pH > 7. Lecourtier and Chauveteau (1990) cautioned interpreting the data at pH  
15 9 > 7 because of possible silica dissolution. Nonetheless, it is generally accepted that with increasing pH beyond  
16 10 the PZC, more and more negative charges become available on the sandstone surface. The estimated values for  
17 11 the surface charge density in this study were in good agreement with the observation of Behrens and Grier (2001)  
18 12 who estimated the surface charge density of a silica sample.

### 19 13 *3.2 Colloidal stability of hematite particles*

20 14 To study the colloidal stability of hematite particles, first, their zeta potential at various pH was measured in  
21 15 a medium with very low ionic strength ( $I = 1$  mM, equivalent to 60 ppm NaCl). As shown in Figure 6, , the PZC  
22 16 of hematite particles was approximately 8.5 in good agreement with measurements reported by others (Kosmulski  
23 17 et al., 2016; Plaza et al., 2010). At pH values above the PZC, the zeta potential values of the particles became  
24 18 more negative, reaching values close to -22 mV at pH 12. The measured zeta potential and PZC of the hematite  
25 19 particles agree well with values reported in the literature (He et al., 2008; Kosmulski, 2002, 2006; Nattich-Rak et  
26 20 al., 2012; Xu et al., 2015; Zhou et al., 2014).

27 21 The relative contributions of the surface forces to particles interactions were predicted by estimating the van  
28 22 der Waals and electrostatic potentials using the DLVO theory (see Section 2.5). Moreover, as will be seen below,  
29 23 the calculations provide insights needed to choose an appropriate ionic strength and pH for the hematite  
30 24 suspension used in the core-floods . For this purpose, the colloidal stability of hematite particles was studied by  
31 25 varying (a) ionic strength and (b) pH. As shown in Equation 4, to estimate the van der Waals potential, the  
32 26 Hamaker constant for hematite ( $A_H$ ) must be known. The Hamaker constant for hematite particles interacting with  
33 27 each other across the water, as the medium, can be calculated from the Lifshitz theory, assuming small differences  
34 28 in dielectric and magnetic properties (Faure et al., 2011). A Hamaker constant of  $25 \times 10^{-20}$  J was used for the  
35 29 DLVO calculations in this study (Rohem Peçanha et al., 2019). The list of other parameters used in the calculations  
36 30 is given in Table S1 in the supplementary materials.

1  
2  
3  
4  
5  
6  
7  
8  
9  
10  
11  
12  
13  
14  
15  
16  
17  
18  
19  
20  
21  
22  
23  
24  
25  
26  
27  
28  
29  
30  
31  
32  
33  
34  
35  
36  
37  
38  
39  
40  
41  
42  
43  
44  
45  
46  
47  
48  
49  
50  
51  
52  
53  
54  
55  
56  
57  
58  
59  
60  
61  
62  
63  
64  
65

Figure 7a shows the total inter-particle interaction potential as a function of particle separation distance for hematite particles at pH 5.8 by varying the ionic strength. At very low ionic strength ( $I = 1$  mM), the potential barrier was approximately  $110/k_B T$ . This implies that colloidal stability is ensured. Nonetheless, increasing the ionic strength to 50, 85 and 200 mM led to a potential barrier smaller than  $16/k_B T$  implying that the colloidal stability is not achieved. It should be noted that  $I = 85$  mM is equivalent to 5,000 ppm NaCl solution which is used to saturate the core prior to injection of hematite suspension.

The effect of pH on the colloidal stability of hematite particles was investigated by varying the pH from 4 to 12. As can be seen in Figure 7b, for pH 4, 5.8, and 12 the potential barrier is larger than  $16/k_B T$ ; however, for pH 8 and 10 the potential barrier was found to be smaller than  $16/k_B T$ . This is attributed to the density of charges on the surface of hematite particles. At pH close to the PZC of hematite particles, the density of charges is low and the van der Waals potential is dominant over the electrostatic potential. Nonetheless, at pH far away from PZC, as it is also evident from zeta potential measurements, the charges density is high enough to make the electrostatic potential larger than the van der Waals potential. This ensures the colloidal stability of hematite particles. The change in colloidal stability as a function of pH is also noticeable from visual inspection and PSD measurement (see Figure S2 and S3 in the supplementary materials which shows the suspension of hematite particles at various pH and their PSD respectively) and only the suspensions with pH far away from the PZC are colloiddally stable.

### 3.3 Deposition of hematite particles in porous media

Based on the results of the above analysis of stability of the suspension of hematite colloidal particles, we chose to work with hematite particles dispersed in [deionized water](#) at pH 5.8 as it indicated sufficient colloidal stability. As hematite particles have a strong tendency to aggregate and form larger particles even in a very short time scale (He et al., 2008), the suspension was continuously stirred prior to injection to the core.

We injected suspensions with hematite concentration of 250 ppm in [deionized water](#) into the core which was saturated with 5000 ppm NaCl solution. It should be noted that with such approach pH and salinity are changed simultaneously. Although the initial contact of the suspension with brine could theoretically have provoked aggregation of hematite particles at the sample inlet, we did not detect any feasible indication of its occurrence. This can be explained by too little ion diffusion speed relative to the speed of the water front propagation. In any case, the possible particle flocculation at the initial phase of the test does not affect our further interpretation and conclusions regarding the effect of pH increase.

1  
2  
3  
4  
5  
6  
7 1 The estimated charge density shown in Figure 8 reveals that in the pH ranging from  $3.4 \pm 0.1$  to  $8.5 \pm 0.1$ ,  
8  
9 2 the hematite and rock surface have opposite charges and consequently their interaction between the particles and  
10 3 rock surface is dominated by electrostatic attraction whereas at  $\text{pH} > 8.5 \pm 0.1$  it is mainly by electrostatic  
11 4 repulsion. Therefore, by the injection of [deionized water](#)-based suspension with pH 5.8, the interaction between  
12 5 particles and pore walls can be expected to be dominated by an electrostatic attraction.  
13  
14

15 6 Flooding with [deionized water](#)-based suspension triggered predictable in-situ clay particles detachment and  
16 7 migration due to salinity drop. Even though clay represented only less than 1 wt% of the dry sandstone, their  
17 8 presence was visually detected in the effluent as a turbidity, sampled during the first 2 PV injected (see Figure S4  
18 9 in the supplementary materials). Since the transparency of the effluent was restored upon injection of 5 PV, for  
19 10 the overall interpretation of the experiments we consider that such low clay content does not influence the results  
20 11 of the study.  
21  
22  
23  
24

25 12 In our experiments, it was observed that hematite nanoparticles affect permeability mainly in the porous  
26 13 medium near the inlet of the samples. Figure 9 shows the differential pressures obtained in Exp. 1. The differential  
27 14 pressure in the first section rose above other sections consistently with the build-up of a filter cake due to a higher  
28 15 amount of particles retained and then increased almost linearly. The filter cake observed at the core inlet after the  
29 16 experiments is shown in Figure 10. On the other hand, a successively smaller permeability decrease was observed  
30 17 in the middle and outlet section of the cores. Upon injection of 32 PV in Exp. 1 and 14 PV in the second one,  
31 18 hematite particles appeared in the effluent (see Figure S4 in the supplementary material). Their concentration in  
32 19 the effluent consistently increased in both tests until the end of hematite suspension injection (60 PV in  
33 20 Experiment 1 and 30PV in the second). Different time of filter cake build-up and particles penetration to the outlet  
34 21 is attributed to the difference in the core properties, permeability in particular.  
35  
36  
37  
38  
39

40 22 The formation of the external filter cake could occur due to electrostatic retention of positively charged  
41 23 hematite particles by negatively charged quartz matrix. [Although at later stages of deposition, when quartz surfaces  
42 24 got considerably covered by hematite particles, they could produce lateral repulsion effects \(Kobayashi et al.,  
43 25 2014\) screening the electrostatic attraction of quartz surfaces.](#) At this stage size-exclusion interception of hematite  
44 26 micro-aggregates, formed in the suspension, could become dominant. It is believed that size-exclusion occurs if  
45 27 infiltrated fines size exceeds 1/6 of the mean pore diameter (Civan, 2016). The contact of [deionized water](#)-based  
46 28 suspension with NaCl brine during its initial displacement could contribute to the aggregation of hematite particles  
47 29 at the core inlet. However, ion diffusion speed was theoretically predicted to be several orders of magnitude lower  
48  
49  
50  
51  
52  
53  
54  
55  
56  
57  
58  
59  
60  
61  
62  
63  
64  
65

1  
2  
3  
4  
5  
6  
7 1 than the speed of concentration front propagation into the core and in our opinion this effect has negligible  
8  
9 2 influence on the results of our study.

10 3 Analysis of CT-derived hematite concentration along the core during the suspension injection confirmed  
11 4 gradual propagation of the particles through the core, although their maximum concentration occurred within the  
12 5 external filter cake at the inlet surface of the cores (Figure 11). At the horizontal axis of the graph, zero coordinate  
13 6 corresponds to the inlet surface of the sample, negative coordinates correspond to the accumulating external filter  
14 7 cake, and positive coordinates correspond to measurements within the core. The CT-derived particles distribution  
15 8 along the samples was in agreement with high-resolution images of the sample slab along its length, made upon  
16 9 completing the flooding tests (Figure 12). Saturation of the reddish color, the characteristic of hematite particles,  
17 10 was maximum at the inlet side (left) of the cores and gradually decreased towards their outlet sides (right).

#### 23 11 3.4 Mobilization of hematite fine particles by pH increase

24 12 Upon completing the injection of the hematite suspension, the core was subjected to flooding with deionized  
25 13 water of increasingly higher pH to initiate hematite particles transport inside the porous medium. The change in  
26 14 differential pressure upon switching from suspension to deionized water observed in Figure 9 was caused by the  
27 15 reduction of the flow rate from 25 mL/min to 10 mL/min. In Exp. 1, the flooding with water with the pH increasing  
28 16 from 7 to 9 caused a gradual rise of differential pressure and consequent decrease of permeability within the inlet  
29 17 sections. In Exp. 2, the rise of differential pressure at same pH levels was noticeably higher. Slight differential  
30 18 pressure rise was also observed within the middle and outlet sections during Exp. 2. The build-up of the differential  
31 19 pressure in the inlet sections is believed to be mainly caused by compaction of the filter cake under the  
32 20 hydrodynamic pressure as well as possible partial flushing particles into the rock and increased clogging of pore  
33 21 throats within the core inlet section. The more pronounced pressure raise in the middle and outlet sections of the  
34 22 second core can be attributed to either penetration of hematite particles or migration of in-situ clays that may  
35 23 disperse from sand grains due to treatment with low concentrated NaOH, that was used for adjusting the pH of  
36 24 the fluids (Osipov 1979).

37 25 The increase of the injected water pH from 9 to 10 in Experiment 1 resulted in differential pressure decline  
38 26 within the inlet section. The differential pressure continuously decreased during the injection of the first 5 PV and  
39 27 stabilized upon the injection of 6 PV (Figure 9). Differential pressure in the middle and outlet section of the core,  
40 28 on the other hand, started slightly rising after 5 PV injected. However, in both tests no hematite presence was  
41  
42  
43  
44  
45  
46  
47  
48  
49  
50  
51  
52  
53  
54  
55  
56  
57  
58  
59  
60  
61  
62  
63  
64  
65

1  
2  
3  
4  
5  
6  
7 1 detected in the effluent, meaning that all released particles were still retained within the core even after the  
8  
9 2 injection of a large number of PVs.

10 3 Further increase in the pH of the injected deionized water from 9 to 11 in Exp. 2 resulted in a steep decrease  
11  
12 4 in the differential pressure drop in the inlet section of the core (Figure 9). Pressure in the middle and outlet sections  
13  
14 5 remained unchanged. Further increase of pH from 11 to 12 resulted in a consistent decline of the differential  
15  
16 6 pressure in the inlet section and a much less pronounced rise of differential pressure in the middle and outlet  
17  
18 7 sections of the core. The differential pressure decline in the inlet section persisted even upon injection of 10 PV  
19  
20 8 while rising asymptotically to a final value in the middle and outlet sections. The observed pressure response to  
21  
22 9 the pH increase in the middle and outlet sections in both tests was much less than in the inlet section, because the  
23  
24 10 most injected colloidal particles were retained at the core inlet surface or within the first section.

25 11 The concentration of particles inside the core was monitored at different stages of both tests with CT-scan.  
26  
27 12 Analysis of the CT-data showed that up to the PZC of hematite particles, the signal from the filter cake was  
28  
29 13 increasing (see Figure S5 in supplementary materials). This is in agreement with differential pressure data that  
30  
31 14 indicated consolidation of the filter cake under the hydrodynamic force. After pH increased above the PZC CT-  
32  
33 15 derived concentration profiles confirmed the decrease of particle concentration in the inlet core section. It should  
34  
35 16 be mentioned that care must be taken to minimize unavoidable artifacts associated with CT scanning to perform  
36  
37 17 reliable quantitative analysis.

#### 38 18 **4. General discussion**

39 19 The purpose of this work was to study the effect of pH alteration on entrapment and remobilization of  
40  
41 20 hematite colloidal particles in porous media. We investigated the charge reversal of the particles above their point  
42  
43 21 of zero charge as a technique to remobilize the deposited particles and transport them in porous media.

44 22 The retention of particles and their further transport was primarily observed by the differential pressure  
45  
46 23 measurements at different lengths of the core. During the hematite deposition stage, the pressure data suggested  
47  
48 24 subsequent deposition of the particles in all sections of the core and formation of a filter cake in the inlet section.  
49  
50 25 Injection of deionized water with pH lower than the point of zero charge of hematite particles (i.e.  $\text{pH } 8.5 \pm 0.1$ )  
51  
52 26 did not trigger any particles migration as the electrostatic interaction between positively charged hematite particles  
53  
54 27 and negatively charged quartz grains of the rock matrix surface was attractive. Injection of deionized water at pH  
55  
56 28 9, which is slightly above the point of zero charge of hematite particles, also did not cause particles mobilization  
57  
58 29 suggesting that the density of negative charges on the particles surface was not high enough to ensure an adequate  
59  
60 30 electrostatic repulsion between particles and rock matrix surface that cause detachment of particles (see Figure 8  
61  
62  
63  
64  
65

1  
2  
3  
4  
5  
6  
7 1 for surface charge density of hematite particles and rock matrix at various pH). Increasing pH to 10, however, led  
8  
9 2 to a decrease of differential pressure in the inlet section and its build-up downstream, indicating the start of the  
10 3 migration of the particles from the inlet surface further inside the core. Further increase in pH, according to the  
11 4 surface charge measurements, led to giving rise to a larger electrostatic repulsion term due to the increase of  
12 5 surface charge density of both hematite and quartz particles. The increase in surface charge density could also  
13 6 contribute to the deflocculation of hematite aggregates formed at the core inlet and penetration of the dispersed  
14 7 particles into the rock. However, the permeability restoration occurred only partially which suggests that the size-  
15 8 exclusion retention of the coagulated hematite particles remained, while the electrostatic retention was eliminated.  
16 9 Analysis of the CT-derived concentration profiles of the hematite also showed the migration of the particles  
17 10 associated with increasing pH.

18 11 The observed results prove the premise that above the point of zero charge, hematite particles came into  
19 12 repulsive interaction with the rock matrix surface which resulted in their detachment and further penetration into  
20 13 the core. However, we found that apart from the sign, the density of charges also plays an important role and at  
21 14 pH values higher but close to the point of zero charge, the density of negative charges on the surface of particles  
22 15 was too small to cause their remobilization.

23 16 The discussed hypothesis was previously reviewed in several studies. In the work of Vaidya and Fogler  
24 17 (1992) migration of in-situ kaolinite particles was observed as a function of pH and severe [permeability](#)  
25 18 [impairment](#) was observed after the charge reversal of the particles due to particles mobilization. A more recent  
26 19 work of Mahmoudi et al. (2016) also observed kaolinite migration in the sandstone at high pH values. In both  
27 20 these studies change of salinity and pH conditions were performed and observed simultaneously whereas in our  
28 21 study we analyzed the influence of pH only. Generally, our work is in agreement with the aforementioned studies  
29 22 on the hypothesis of mobilization of particles with a pH-dependent surface charge at a high pH level. [As the step](#)  
30 23 [forward in the ongoing research we provide a detailed theoretical study of colloidal stability of hematite particles](#)  
31 24 [and report the effect of surface charge density of particles and rock matrix on the electrostatic interaction between](#)  
32 25 [them. Moreover, we experimentally established the theoretical possibility of external particles remobilization and](#)  
33 26 [migration because of their charge reversal caused by pH increase, by means of variety of methods, including CT](#)  
34 27 [scanning technique that proved to be an effective tool for monitoring the migration of colloidal particles in the](#)  
35 28 [porous media throughout the experiment.](#)

36 29 The following limitations of this work must be acknowledged. The strong tendency of hematite colloidal  
37 30 particles to aggregate needs to be taken into account in all stages of the particles characterization and core-flood  
38  
39  
40  
41  
42  
43  
44  
45  
46  
47  
48  
49  
50  
51  
52  
53  
54  
55  
56  
57  
58  
59  
60  
61  
62  
63  
64  
65

1  
2  
3  
4  
5  
6  
7 1 experiments. For instance, particles tend to sediment shortly after preparation, therefore the analysis of their  
8  
9 2 particle size distribution, determined by dynamic light scattering, should be done with caution. Besides,  
10 3 limitations of CT scanning include minimization of experimental artifacts for the quantitative analysis. These  
11 4 artifacts can appear on CT images as an effect of the core position inside the scanner and selected scanning  
12 5 parameters and they need to be minimized at the preparation stage and during image analysis. Also, the  
13 6 interpretation of the core-flood experiments in our study was primarily focused on the interactions between  
14 7 particles and rock surface. Further theoretical studies which include both rock-particle and particle-particle  
15 8 interactions are recommended.

19 9 As mentioned before, hematite particles were chosen for the study specifically because they have pH-  
20 10 dependent surface charge and are traceable under CT scan. However, we believe that the conclusions of this study  
21 11 can be extrapolated to real field-case applications of natural clastic reservoirs. The main mineral of such reservoirs  
22 12 is quartz, similar to the rock in our studies. Since the point of zero charge of quartz is lower than the naturally  
23 13 occurring pH, the sand grains surfaces are usually negatively charged in clastic reservoirs. Clay minerals, usually  
24 14 presented in the natural rocks, have very different and complex mineralogy and crystal structure, therefore their  
25 15 PZC can vary significantly. At the same time clay minerals, similar to colloidal particles of hematite used in this  
26 16 study, are hydrated in water and therefore respond to the changes in the surrounding environment. At naturally  
27 17 occurring pH clay particles are electrostatically attracted to quartz grains and an increase in pH can reverse their  
28 18 surface charge and initiate migration, as it was shown in the works mentioned above (Mahmoudi et al., 2016;  
29 19 Vaidya & Fogler, 1992). Therefore, we suggest that the mechanism of particle charge reversal due to an increase  
30 20 of pH over the PZC can result in the same behavior for clay minerals in the natural clastic rocks and other minerals  
31 21 with pH-dependent surface charge. This suggestion is a foundation for further detailed and comparative research.

## 39 22 **5. Conclusions**

41 23 In this work, the impact of pH alteration on entrapment and remobilization of hematite particles in a sandstone  
42 24 porous medium was investigated. The experiments showed that the rock surface was negatively charged at pH  
43 25 values higher than ~3.4 while the surface of hematite particles became negatively charged only at pH values  
44 26 higher than ~8.5. Injection of the hematite suspension at original pH 5.8 into the sandstone core led to the  
45 27 formation of a filter cake in the inlet due to the combined effect of electrostatic retention of positively charged  
46 28 hematite particles on negatively rock surface and size-exclusion interception of hematite micro-aggregates formed  
47 29 in the suspension. During the injection of [deionized water](#) with pH values up to 9, no indication of hematite  
48 30 particles mobilization in the filter cake was observed. At pH values higher than 9, however, a decrease of  
49  
50  
51  
52  
53  
54  
55  
56  
57  
58  
59  
60  
61  
62  
63  
64  
65



1  
2  
3  
4  
5  
6  
7 1 differential pressure in the inlet section was noticed, indicating the start of the migration of the particles from the  
8 2 inlet surface further inside the core and partial destruction of the filter cake. This was due to a change of surface  
9 3 charge of hematite particles from positive to negative giving rise to a repulsion term when they interact with  
10 4 negatively charged rock surface which ceases electrostatic retention of hematite particles and enables their further  
11 5 penetration into the rock porous network. Analysis of the CT-derived concentration profiles also showed the  
12 6 decrease of particle concentration in the inlet core section at pH values higher than 9. The results of this study  
13 7 provide insights into fine-tuning the electrostatic interactions in porous media and thus mitigating the [permeability](#)  
14 8 [reduction](#) as a result of fines migration for particles with pH-dependent surface charge.

#### 19 9 **Acknowledgements**

20  
21 10 This work was supported by the Ministry of Science and Higher Education of the Russian Federation  
22 11 under agreement No. 075-15-2020-119 within the framework of the development program for a world-class  
23 12 Research Center. We thank the Ministry of Science and Higher Education of the Russian Federation for its  
24 13 support.

25  
26  
27 14 The authors gratefully acknowledge the Skolkovo Institute of Science and Technology (Russia) and Delft  
28 15 University of Technology (The Netherlands) for providing their laboratories facilities for the experiments. The  
29 16 authors thank Michiel Slob, Jolanda van Haagen, Marc Friebe, and Ellen Meijvogel-de Koning for technical  
30 17 support. The authors also acknowledge Martijn Janssen, Swej Shah, and Sian Jones for fruitful discussions.

31  
32  
33  
34  
35  
36  
37  
38  
39  
40  
41  
42  
43  
44  
45  
46  
47  
48  
49  
50  
51  
52  
53  
54  
55  
56  
57  
58  
59  
60  
61  
62  
63  
64  
65

**References**

1. Aji, K., You, Z., Badalyan, A., & Bedrikovetsky, P. (2012). Study of particle straining effect on produced water management and injectivity enhancement. *SPE International Production and Operations Conference and Exhibition, Doha Qatar*, (May), 14–16.
2. Al-Sarihi, A., Zeinjahromi, A., Genolet, L., Behr, A., Kowollik, P., & Bedrikovetsky, P. (2018). Effects of Fines Migration on Residual Oil during Low-Salinity Waterflooding. *Energy & Fuels*, 32(8), 8296-8309. doi:10.1021/acs.energyfuels.8b01732
3. Al-Yaseri, A. Z.; Lebedev, M.; Vogt, S. J.; Johns, M. L.; Barifcani, A.; Iglauer, S. (2015) Pore-scale analysis of formation damage in Bentheimer sandstone with in-situ NMR and micro-computed tomography experiments. *Journal of Petroleum Science and Engineering*, 129, 48-57.
4. Alexandrino, J. S., Peres, A. E. C., Lopes, G. M., & Rodrigues, O. M. S. (2016). Dispersion degree and zeta potential of hematite. *Revista Escola de Minas*, 69(2), 193–198. <https://doi.org/10.1590/0370-44672014690073>.
5. Alshakhs, M. J., & Kovscek, A. R. (2016). Understanding the role of brine ionic composition on oil recovery by assessment of wettability from colloidal forces. *Advances in Colloid and Interface Science*, 233, 126-138. doi:<https://doi.org/10.1016/j.cis.2015.08.004>
6. Alvarez-Silva, M., Mirnezami, M., Uribe-Salas, A., & Finch, J. A. (2010). Point of Zero Charge , Isoelectric Point and Aggregation of Phyllosilicate Minerals. *Canadian Metallurgical Quarterly*, 49, 405–410. <https://doi.org/10.1179/cmq.2010.49.4.405>.
7. Austad, T.; RezaeiDoust, A.; Puntervold, T. (2010). Chemical mechanism of low salinity water flooding in sandstone reservoirs. *SPE improved oil recovery symposium; Society of Petroleum Engineers: Richardson, TX, USA*; DOI: 10.2118/129767-MS.
8. Barouch, E., Wright, T. H., & Matijević, E. (1987). Kinetics of particle detachment: I. General considerations. *Journal of Colloid and Interface Science*, 118(2), 473-481. doi:[https://doi.org/10.1016/0021-9797\(87\)90483-8](https://doi.org/10.1016/0021-9797(87)90483-8)
9. Behrens, S. H.; Grier, D. G. (2001). The charge of glass and silica surfaces. *The Journal of Chemical Physics*, 115, (14), 6716-6721.
10. Berg, J. C. (2010). *An Introduction to Interfaces & Colloids the Bridge to Nanoscience*; World Scientific Publishing Co. Pte. Ltd: Singapore.

11. Borazjani, S., Kulikowski, D., Amrouch, K., & Bedrikovetsky, P. (2018). Composition changes of hydrocarbons during secondary petroleum migration. *The APPEA Journal*, 58, 784. doi:10.1071/AJ17127
12. Byrne, M., Patey, I., & Green, J. (2007). A New Tool for Exploration and Appraisal-Formation Damage Evaluation.
13. Churcher, P. L., French, P. R., Shaw, J. C., & Schramm, L. L. (1991). Rock Properties of Berea Sandstone, Baker Dolomite, and Indiana Limestone. *SPE International Symposium on Oilfield Chemistry, Anaheim, California*, (January), 431–446. <https://doi.org/10.2118/21044-MS>
14. Civan F. (2016) *Reservoir Formation Damage. 3rd edition.* Elsevier Inc. <https://doi.org/10.1016/B978-0-12-801898-9.00028-X>
15. Dahneke, B. (1975). Resuspension of particles. *Journal of Colloid and Interface Science*, 50(1), 194-196. doi:[https://doi.org/10.1016/0021-9797\(75\)90266-0](https://doi.org/10.1016/0021-9797(75)90266-0)
16. Darcy, H. (1856). Les Fontaines Publiques de la Ville de Dijon, Dalmont, Paris.
17. Davis, J. A.; James, R. O.; Leckie, J. O. (1978). Surface ionization and complexation at the oxide/water interface: I. Computation of electrical double layer properties in simple electrolytes. *Journal of Colloid and Interface Science*, 63, (3), 480-499.
18. Dickson, D., Liu, G., Li, C., Tachiev, G., & Cai, Y. (2012). Dispersion and stability of bare hematite nanoparticles: effect of dispersion tools, nanoparticle concentration, humic acid and ionic strength. *Science of the Total Environment*, 419, 170–177. <https://doi.org/10.1016/j.scitotenv.2012.01.012>.
19. Didier, M., Chaumont, A., Joubert, T., Bondino, I., & Hamon, G. (2015). Contradictory trends for smart water injection method: role of pH and salinity from sand/oil/brine adhesion maps. *International Symposium of the Society of Core Analysts*, 12.
20. Elimelech, M., Gregory, J., Xia, X., Williams, R.A. (1995). *Particle Deposition and Aggregation*, paperback ed., Butterworth-Heinemann, Oxford.
21. Elimelech, M. (1991). Kinetics of capture of colloidal particles in packed beds under attractive double layer interactions, *J. Colloid Interf. Sci.* 146, 337–352.
22. Farooq, U.; Tweheyo, M. T.; Sjöblom, J.; Øye, G. (2011) Surface Characterization of Model, Outcrop, and Reservoir Samples in Low Salinity Aqueous Solutions. *Journal of Dispersion Science and Technology*, 32, (4), 519-531.
23. Faure, B.; Salazar-Alvarez, G.; Bergström, L. (2011). Hamaker Constants of Iron Oxide Nanoparticles. *Langmuir*, 27, (14), 8659-8664.

- 1  
2  
3  
4  
5  
6  
7 1 24. He, Y. T., Wan, A. J., & Tokunaga, At. (2008). Kinetic stability of hematite nanoparticles : the effect of  
8  
9 2 particle sizes. *The Journal of Nanoparticle Research*, 10, 321–332. [https://doi.org/10.1007/s11051-007-](https://doi.org/10.1007/s11051-007-9255-1)  
10 3 9255-1  
11  
12 4 25. Hotze, E. M.; Phenrat, T.; Lowry, G. V. (2010). Nanoparticle aggregation: challenges to understanding  
13  
14 5 transport and reactivity in the environment. *J Environ Qual*, 39, (6), 1909-24.  
15 6 26. Iglauer, S., Favretto, S., Spinelli, G., Schena, G., & Blunt, M. J. (2010). X-ray tomography measurements  
16 7 of power-law cluster size distributions for the nonwetting phase in sandstones. *Phys Rev E Stat Nonlin Soft*  
17 8 *Matter Phys*, 82(5 Pt 2), 056315. doi:10.1103/PhysRevE.82.056315  
19 9 27. Israelachvili, J. (2011). *Intermolecular and Surface Forces 3rd Edition*. Academic Press.  
21 10 28. Jung, J. W., Jang, J., Santamarina, J. C., Tsouris, C., Phelps, T. J., & Rawn, C. J. (2012). Gas Production  
22 11 from Hydrate-Bearing Sediments: The Role of Fine Particles. *Energy & Fuels*, 26(1), 480-487.  
23 12 doi:10.1021/ef101651b  
25 13 29. Kalantariasl, A., & Bedrikovetsky, P. (2014). Stabilization of External Filter Cake by Colloidal Forces in a  
26 14 “Well–Reservoir” System. *Industrial & Engineering Chemistry Research*, 53(2), 930-944.  
27 15 doi:10.1021/ie402812y  
30 16 30. Katende, A., & Sagala, F. (2019). A critical review of low salinity water flooding: Mechanism, laboratory  
31 17 and field application. *Journal of Molecular Liquids*, 278, 627–649.  
32 18 <https://doi.org/10.1016/j.molliq.2019.01.037>  
34 19 31. Kia, S. F., Fogler, H. S., & Reed, M. G. (1987). Effect of pH on colloiddally induced fines migration. *Journal*  
35 20 *of Colloid and Interface Science*, 118(1), 158-168. doi:[https://doi.org/10.1016/0021-9797\(87\)90444-9](https://doi.org/10.1016/0021-9797(87)90444-9)  
36 21 [32.](#) Kia, S. F., Fogler, H. S., Reed, M. G., & Vaidya, R. N. (1987). Effect of Salt Composition on Clay Release  
37 22 in Berea Sandstones. *SPE Production Engineering*, 2(04), 277-283. doi:10.2118/15318-PA  
38 23 [33.](#) Kobayashi, M., Nanaumi, H., Muto, Y. (2009). Initial deposition rate of latex particles in the packed bed of  
39 24 [zirconia beads. Colloids and Surfaces A: Physicochem. Eng. Aspects, 347, 2-7.](#)  
40 25 [32-34.](#) Kobayashi, M., Ookawa, M., Yamada, S. (2014) The effects of surface charging properties on colloid  
41 26 [transport in porous media. Applied Mechanics J., vol.17, 743-752.](#)  
42 27 [33-35.](#) Kolakowski, J. E., & Matijević, E. (1979). Particle adhesion and removal in model systems. Part 1.—  
43 28 Monodispersed chromium hydroxide on glass. *Journal of the Chemical Society, Faraday Transactions 1:*  
44 29 *Physical Chemistry in Condensed Phases*, 75(0), 65-78. doi:10.1039/F19797500065  
45  
46  
47  
48  
49  
50  
51  
52  
53  
54  
55  
56  
57  
58  
59  
60  
61  
62  
63  
64  
65

- 1  
2  
3  
4  
5  
6  
7 1 [34-36.](#) Kosmulski, M. (2002) The pH-Dependent Surface Charging and the Points of Zero Charge. *Journal of*  
8 *Colloid and Interface Science*, 253, (1), 77-87.  
9 2
- 10 3 [35-37.](#) Kosmulski, M. (2006). pH-dependent surface charging and points of zero charge III. Update. *Journal of*  
11 *Colloid and Interface Science*, 298, (2), 730-41.  
12 4
- 13 5 [36-38.](#) Kosmulski, M. (2016). Isoelectric points and points of zero charge of metal (hydr)oxides : 50 years after  
14 Parks' review. *Advances in Colloid and Interface Science*, 238, 1–61.  
15 6 <https://doi.org/10.1016/j.cis.2016.10.005>  
16 7
- 18 8 [37-39.](#) Kumar, N., Andersson, M. P., van den Ende, D., Mugele, F., & Siretanu, I. (2017). Probing the Surface  
19 Charge on the Basal Planes of Kaolinite Particles with High-Resolution Atomic Force Microscopy.  
20 *Langmuir*, 33(50), 14226-14237. doi:10.1021/acs.langmuir.7b03153  
21 10
- 22 11 [38-40.](#) Lei, H., Dong, L., Ruan, C., & Ren, L. (2017). Study of migration and deposition of micro particles in  
23 porous media by Lattice-Boltzmann Method. *Energy Procedia*, 142, 4004-4009.  
24 12 doi:<https://doi.org/10.1016/j.egypro.2017.12.317>  
25 13
- 27 14 [39-41.](#) Lecourtier, J.; Lee, L. T.; Chauveteau, G. (1990). Adsorption of polyacrylamides on siliceous minerals.  
28 *Colloids and Surfaces*, 47, 219-231.  
29 15
- 30 16 [40-42.](#) Lützenkirchen, J.; Preocanin, T.; Kovačević, D.; Tomišić, V.; Lövgren, L.; Kallay, N. (2012).  
31 Potentiometric Titrations as a Tool for Surface Charge Determination. *Croatica Chemica Acta*, 85, 391-417.  
32 17
- 33 18 [41-43.](#) Mahmoudi, M., Fattahpour, V., Nouri, A., & Leitch, M. (2016). An Experimental Investigation of the  
34 Effect of pH and Salinity on Sand Control performance for heavy oil thermal production. *SPE Canada Heavy*  
35 19 *Oil Technical Conference, Calgary*, (June), 18. <https://doi.org/10.2118/180756-MS>  
36 20
- 38 21 [42-44.](#) McDowell-Boyer, L. M., Hunt, J. R., & Sitar, N. (1986). Particle transport through porous media. *Water*  
39 *Resources Research*, 22(13), 1901-1921. doi:10.1029/WR022i013p01901  
40 22
- 41 23 [43-45.](#) Mietta, F., Chassagne, C., & Winterwerp, J. C. (2009). Shear-induced flocculation of a suspension of  
42 kaolinite as function of pH and salt concentration. *Journal of Colloid and Interface Science*, 336(1), 134-  
43 141. doi:<https://doi.org/10.1016/j.jcis.2009.03.044>  
44 25
- 45 26 [44-46.](#) Mirzaie Yegane, M.; Minaye Hashemi, F. S.; Vercauteren, F.; Meulendijks, N.; Gharbi, R.; Boukany, P.  
46 E.; Zitha, P. L. J. (2020). Rheological response of a modified polyacrylamide – silica nanoparticles hybrid  
47 27 at high salinity and temperature. *Soft Matter*, 16, 10198-10210. doi:[10.1039/d0sm01254h](https://doi.org/10.1039/d0sm01254h)  
48 28
- 50 29 [45-47.](#) Mitchell, J. K. (1993). *Fundamentals of Soil Behavior*. John Wiley & Sons, Inc.  
51 30
- 52 30 [46-48.](#) Moskovits, M.; Vlčková, B. (2005). Adsorbate-Induced Silver Nanoparticle Aggregation Kinetics. *The*  
53  
54  
55  
56  
57  
58  
59  
60  
61  
62  
63  
64  
65

1  
2  
3  
4  
5  
6  
7 1 *Journal of Physical Chemistry B*, 109, (31), 14755-14758.

8  
9 2 [47-49.](#) Nasralla, R. A., Bataweel, M. A., & Nasr-El-Din, H. A. (2013). Investigation of Wettability Alteration  
10 and Oil-Recovery Improvement by Low-Salinity Water in Sandstone Rock. *Journal of Canadian Petroleum*  
11 *Technology*, 52(02), 144-154. doi:10.2118/146322-PA

12 4  
13 5 [48-50.](#) Ohshima, H. (1995). Effective Surface Potential and Double-Layer Interaction of Nanoparticles. *Journal*  
14 *of Colloid and Interface Science*, 174, (1), 45-52.

15 6  
16 7 [49-51.](#) Olphen H. van., (1963). *An introduction to clay colloid chemistry*. Interscience Publications (New York).

17 8  
18 9 [50-52.](#) Osipov V.I., (1979). *Nature of strength and deformation properties of clay rocks*. Moscow, in Russian.

19 10  
20 11 [51-53.](#) Osipov V.I., Sokolov V.N., Rumiantseva N.A., (1989). *Microstructure of clay rocks*. Moscow, Nedra.  
21 In Russian.

22 12  
23 13 [52-54.](#) Peksa, A. E., Wolf, K. H. A. A., Slob, E. C., Chmura, L., & Zitha, P. L. J. (2017). Original and  
24 pyrometamorphical altered Bentheimer sandstone; petrophysical properties, surface and dielectric behavior.  
25 *Journal of Petroleum Science and Engineering*, 149, 270–280. <https://doi.org/10.1016/j.petrol.2016.10.024>

26 14  
27 15 [53-55.](#) Plaza, R. C., González-Caballero, F., & Delgado, A. V. (2001). Electrical surface charge and potential  
28 of hematite/yttrium oxide core-shell nanoparticles. *Colloid and Polymer Science*, 279(12), 1206-1211.  
29 doi:10.1007/s003960100578

30 16  
31 17 [54-56.](#) Pooryousefy, E., Xie, Q., Chen, Y., Sari, A., & Saeedi, A. (2018). Drivers of low salinity effect in  
32 sandstone reservoirs. *Journal of Molecular Liquids*, 250, 396-403.  
33 doi:<https://doi.org/10.1016/j.molliq.2017.11.170>

34 18  
35 19 [55-57.](#) Priisholm, S., Nielson, B.L., Haslund, O. (1987). Fines migration, blocking, and clay swelling of  
36 potential geothermal sandstone reservoirs, Denmark. *SPE Formation Evaluation*, 168-178.  
37 Doi:10.2118/15199-PA

38 20  
39 21 [56-58.](#) Raghavan, S. R.; Hou, J.; Baker, G. L.; Khan, S. A. (2000). Colloidal Interactions between Particles with  
40 Tethered Nonpolar Chains Dispersed in Polar Media: Direct Correlation between Dynamic Rheology and  
41 Interaction Parameters. *Langmuir*, 16, (3), 1066-1077.

42 22  
43 23 [57-59.](#) Rohem Peçanha, E.; da Fonseca de Albuquerque, M. D.; Antoun Simão, R.; de Salles Leal Filho, L.; de  
44 Mello Monte, M. B. (2019). Interaction forces between colloidal starch and quartz and hematite particles in  
45 mineral flotation. *Colloids and Surfaces A: Physicochemical and Engineering Aspects*, 562, 79-85.

46 24  
47 25  
48 26  
49 27  
50  
51  
52  
53  
54  
55  
56  
57  
58  
59  
60  
61  
62  
63  
64  
65

- 1  
2  
3  
4  
5  
6  
7 1 [58-60.](#) Rosenbrand, E., Kjølner, C., Riis, J. F., Kets, F., & Fabricius, I. L. (2015). Different effects of temperature  
8 and salinity on permeability reduction by fines migration in Berea sandstone. *Geothermics*, 53, 225-235.  
9 doi:<https://doi.org/10.1016/j.geothermics.2014.06.004>
- 10 3  
11 4 [59-61.](#) Rostami, A., & Nasr-El-Din, H. (2010). A new technology for filter cake removal. *Society of Petroleum*  
12 *Engineers - SPE Russian Oil and Gas Technical Conference and Exhibition 2010, RO and G 10*, 2(October),  
13 1063–1079.  
14 6
- 15 7 [60-62.](#) Russell, T., Chequer, L., Badalyan, A., Behr, A., Genolet, L., Kowollik, P., Bedrikovetsky, P. (2018).  
16 Systematic laboratory and modelling study of kaolinite in rocks on formation-damage-fines-migration non-  
17 equilibrium effects, analytical model. *Proceedings - SPE International Symposium on Formation Damage*  
18 *Control, 2018-Febru.* <https://doi.org/10.2118/189533-ms>
- 19 9  
20 11 [61-63.](#) Russell, T., Chequer, L., Borazjani, S., You, Z., Zeinijahromi, A., & Bedrikovetsky, P. (2018).  
21 *Formation Damage by Fines Migration : Mathematical and Laboratory Modeling , Field Cases.* Elsevier,  
22 Amsterdam, 69-175. <https://doi.org/10.1016/B978-0-12-813782-6.00003-8>
- 23 12  
24 14 [62-64.](#) Sarkar, A. K., Sharma, M. M. (1990). Fines Migration in Two-Phase Flow. *Journal of Petroleum*  
25 *Technology*, (May), 646–652.  
26 15
- 27 16 [63-65.](#) Schroth, B. K., & Sposito, G. (1997). Surface charge properties of kaolinite. *Clays and Clay Minerals*,  
28 *45(1)*, 85–91.  
29 17
- 30 18 [64-66.](#) Sharma M.M., Yortsos Y.C. (1987) Fines migration in porous media. *AIChE Journal*, 10 (33), 1654–  
31 1662.  
32 19
- 33 20 [65-67.](#) Sheng, J. (2010). *Modern chemical enhanced oil recovery: Theory and practice*; Gulf: Burlington, MA,  
34 USA.  
35 21
- 36 22 [66-68.](#) Skoglund, S.; Lowe, T. A.; Hedberg, J.; Blomberg, E.; Wallinder, I. O.; Wold, S.; Lundin, M. (2013).  
37 Effect of Laundry Surfactants on Surface Charge and Colloidal Stability of Silver Nanoparticles. *Langmuir*,  
38 *29*, (28), 8882-8891.  
39 23
- 40 24 Tadros, T.F. (2014). *General Principles of Colloid Stability and the Role of Surface Forces*. Wiley-VCH  
41 Verlag GmbH & Co. KGaA, 1-22.  
42 25
- 43 26 [67-69.](#) Tchistiakov, A. A. (2000). Colloid chemistry of in-situ clay-induced formation damage. *SPE*  
44 *International Symposium on Formation Damage Control, Lafayette*, 371–379.  
45 27  
46 28  
47 29 <https://doi.org/10.2523/58747-ms>.  
48  
49  
50  
51  
52  
53  
54  
55  
56  
57  
58  
59  
60  
61  
62  
63  
64  
65

- 1  
2  
3  
4  
5  
6  
7 1 [68-70.](#) Tchistiakov, A. (2000). Physico-chemical aspects of clay migration and injectivity decrease of  
8 geothermal clastic reservoirs. *Proceedings World Geothermal Congress*, 3087-3095.  
9 2
- 10 3 [69-71.](#) Tchistiakov, A. (2000). Physico-Chemical Factors Controlling In-Situ Clay-Induced Formation Damage  
11 During Water Re-Injection. *Proceedings of ETCE 2000 & OMAE 2000 Joint Conference Energy for the*  
12 4 *New Millennium*, February 14-17, New Orleans, USA.  
13 5
- 14 6 [70-72.](#) Tchistiakov A. A., Sokolov V.N., Osipov V.I. (2001). Saponite clay tailing treatment by artificial  
15 7 sedimentation. *Clay Science for Engineering*, Adachi & Fukue (eds), Balkema, Rotterdam, ISBN  
16 8 9058091759.  
17 8
- 18 9 [71-73.](#) Torkzaban, S., Bradford, S. A., & Walker, S. L. (2007). Resolving the Coupled Effects of  
19 10 Hydrodynamics and DLVO Forces on Colloid Attachment in Porous Media. *Langmuir*, 23(19), 9652-9660.  
20 11 doi:10.1021/la700995e  
21 12
- 22 12 [72-74.](#) Vaidya, R. N., & Fogler, H. S. (1990). Formation damage due to colloiddally induced fines migration.  
23 13 *Colloids and Surfaces*, 50, 215-229. doi:[https://doi.org/10.1016/0166-6622\(90\)80265-6](https://doi.org/10.1016/0166-6622(90)80265-6)  
24 14
- 25 14 [73-75.](#) Vaidya, R. N., & Fogler, H. S. (1992). Fines migration and formation damage: Influence of pH and ion  
26 15 exchange. *Society of Petroleum Engineers - SPE Production Engineering 1992*, (November), 325-330.  
27 16
- 28 16 [74-76.](#) Wijenayaka, L. A., Ivanov, M. R., Cheatum, C. M., Haes, A. J. (2015). Improved Parametrization for  
29 17 Extended Derjaguin, Landau, Verwey, and Overbeek Predictions of Functionalized Gold Nanosphere  
30 18 Stability. *The Journal of Physical Chemistry C*, 119(18), 10064-10075.  
31 19
- 32 19 [75-77.](#) Xu, C.-y., Deng, K.-y., Li, J.-y., Xu, R.-k. (2015). Impact of environmental conditions on aggregation  
33 20 kinetics of hematite and goethite nanoparticles. *Journal of Nanoparticle Research*, 17(10), 394.  
34 21
- 35 21 [76-78.](#) You, Z., Aji, K., Badalyan, A., & Bedrikovetsky, P. (2012). Effect of nanoparticle transport and retention  
36 22 in oilfield rocks on the efficiency of different nanotechnologies in oil industry. *Society of Petroleum*  
37 23 *Engineers - SPE International Oilfield Nanotechnology Conference 2012*, (June), 397-411.  
38 24 <https://doi.org/10.2118/157097-ms>  
39 25  
40 26  
41  
42  
43  
44  
45  
46  
47  
48  
49  
50  
51  
52  
53  
54  
55  
56  
57  
58  
59  
60  
61  
62  
63  
64  
65



1. Figures and Tables

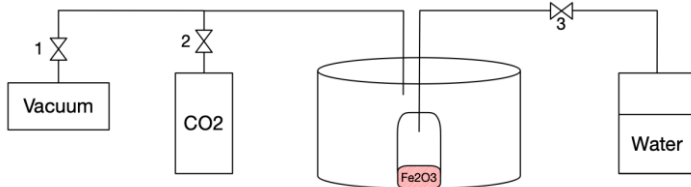


Figure 1 – Setup for preparation of hematite suspension. The hematite powder was vacuumed through valve 1 and CO<sub>2</sub> and water were further added through valves 2 and 3 respectively.

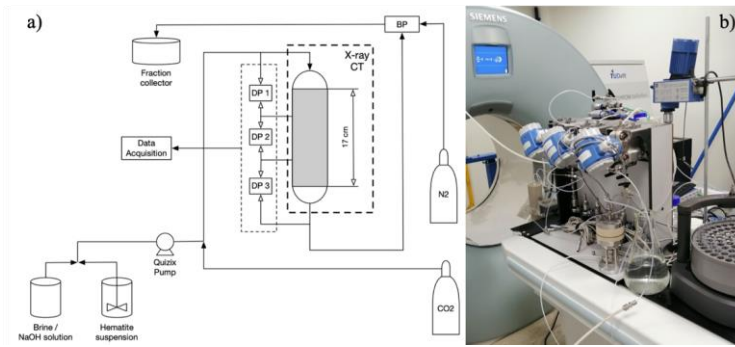


Figure 2 – a) The schematic drawing of the experimental setup used to perform the core-flood experiments. DP = differential pressure, BP = back pressure; b) photo of the setup.

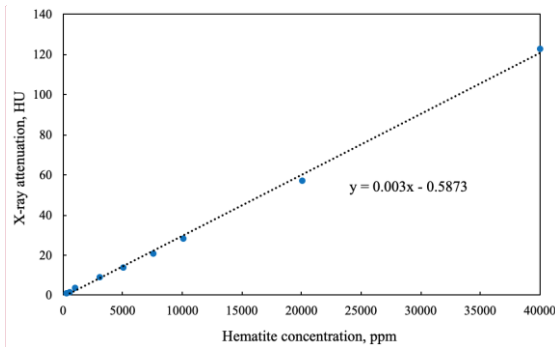


Figure 3 – Calibration curve of CT value as a function of hematite concentration. The concentration ranging from 0 to 40,000 was used. The dashed line represents the linear trend line of the concentration.

Commented [AK1]: Tick marks were added

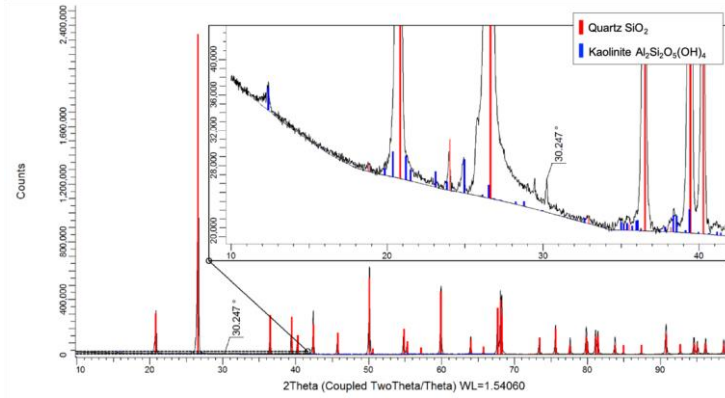


Figure 4 – XRD pattern of the pulverized Bentheimer sample used for Exp.1 1. Based on the semi-quantitative approach, silica was found to be the main compound in the rock ( $99.3 \pm 0.1$  wt%). There was also a small fraction of kaolinite ( $0.7 \pm 0.1$  wt%)

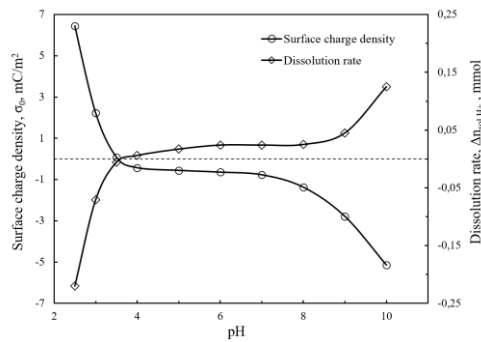


Figure 5 – Estimation of the dissolution rate and surface charge density as a function of pH for the Bentheimer sample used in the core-flood experiments based on the potentiometric mass titration data. Above the  $PZC=3.4 \pm 0.1$ , the rock surface is negatively charged

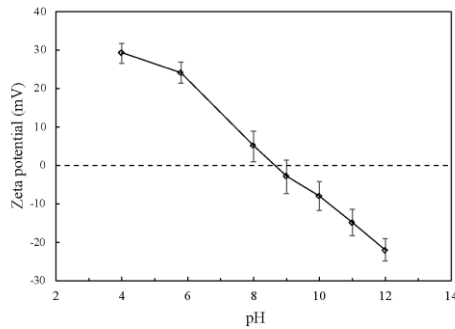


Figure 6 – Zeta potential measurements at various pH to identify the PZC of hematite particles. The PZC was found at  $pH 8.5 \pm 0.1$

Commented [AK2]: Tick marks were added

Commented [AK3]: Tick marks were added

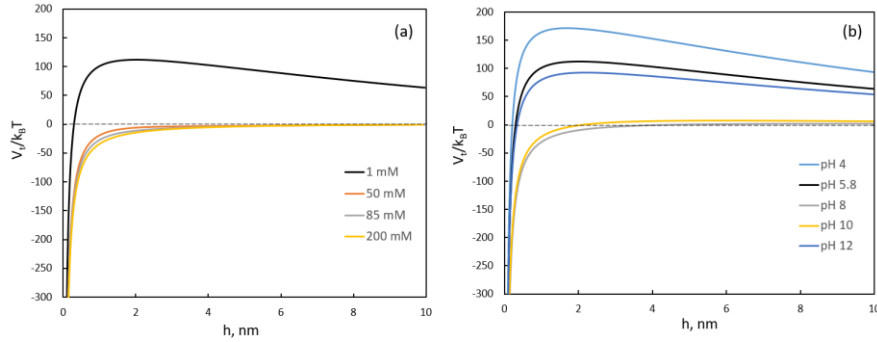


Figure 7 – Inter-particle interaction potential ( $V_i$ ) as a function of particle separation distance ( $h$ ) calculated by DLVO theory: a) Effect of ionic strength on hematite particle interaction at pH 5.8; b) Effect of pH on hematite particle interaction at  $I = 1$  mM using zeta potential values given in Figure 6

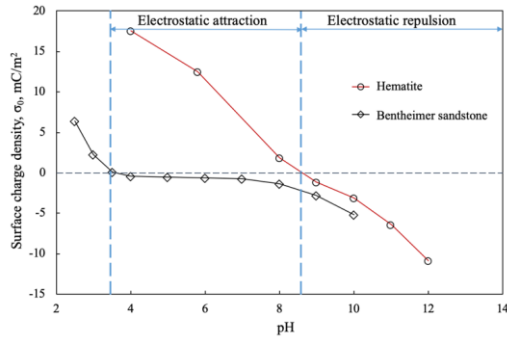


Figure 8 – The estimated surface charge density for the hematite particles and the Bentheimer sample used in the core-flood experiments. In the pH ranging from  $3.4 \pm 0.1$  to  $8.5 \pm 0.1$ , the interaction between the particles and rock surface is dominated by the electrostatic attraction whereas at  $pH > 8.5 \pm 0.1$  is dominated by electrostatic repulsion.

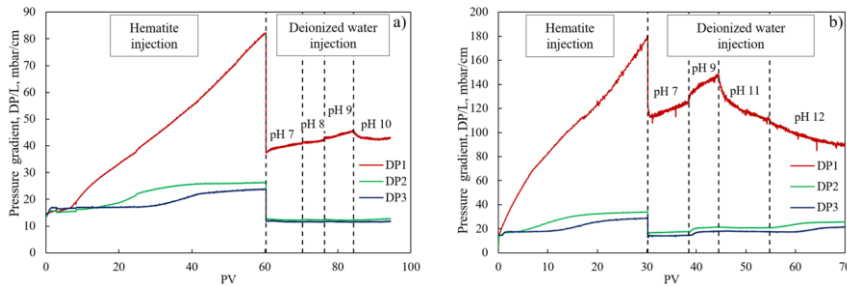


Figure 9 – Pressure gradient as the function of PV injected during core-flood experiments in three sections of the core: a) Exp. 1, injection of hematite suspension and deionized water with pH 7-10, b) Exp. 2 injection of hematite suspension and deionized water with pH 7-12

Commented [AK4]: Tick marks were added, x-axis was moved. Figure 7a was modified

Commented [AK5]: Tick marks were added, x-axis was moved

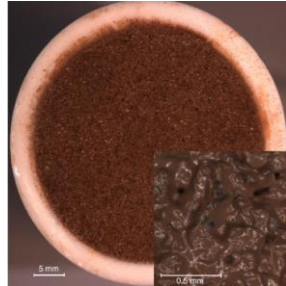
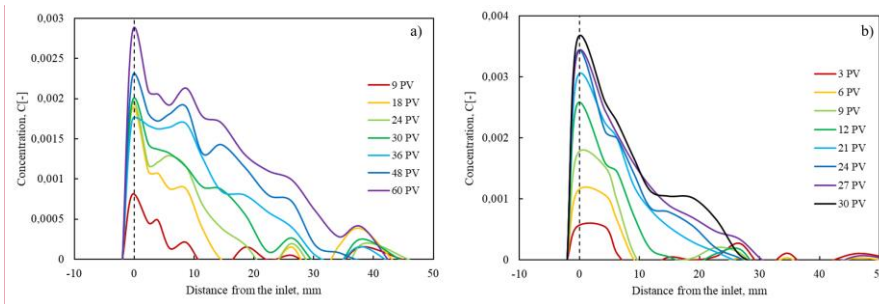


Figure 10 – Filter cake observed at the core inlet as a result of injection of hematite suspension (Exp. 1)



Commented [AK6]: Tick marks were added

Figure 11 – Hematite concentration as a function of distance from core inlet: a) Exp. 1, from 9 PV to 60 PV, b) Exp. 2, from 3 PV to 30 PV. All the data shown correspond to section 1 of the cores.

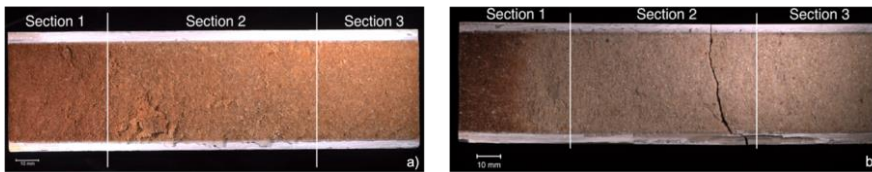


Figure 12 –Microscopic image of the core after core-flood experiments: a) Exp. 1, b) Exp. 2.

Table 1 – Properties of Bentheimer core samples

| Components           | Quartz         | Kaolinite     |
|----------------------|----------------|---------------|
|                      | 99.3 ± 0.1 wt% | 0.7 ± 0.1 wt% |
| Porosity             | 24.4 ± 0.2 %   |               |
| Initial Permeability | Exp. 1         | Exp. 2        |
|                      | 1770 ± 20 mD   | 1400 ± 20 mD  |

Darcy (D) - permeability of the porous medium through which the flow of 1cm<sup>3</sup> of fluid with viscosity of 1 cp in 1 sec under the differential pressure of 1 atm, where the porous medium has cross-sectional area of 1 cm<sup>2</sup> and length of 1 cm. 1 mD ≈ 1 μm<sup>2</sup>·10<sup>-3</sup>.

Table 2 – Parameters of the experiments

|        | Permeability | Stage 1             | Stage 2                | Stage 3       | Stage 4       | Stage 5       |
|--------|--------------|---------------------|------------------------|---------------|---------------|---------------|
| Exp. 1 | 1770 ± 20 mD | Hematite suspension | <u>Deionized water</u> |               |               |               |
|        |              |                     | pH 7                   | pH 8          | pH 9          | pH 10         |
|        |              | Q = 25 mL/min       | Q = 10 mL/min          | Q = 10 mL/min | Q = 10 mL/min | Q = 10 mL/min |
|        |              | V = 60 PV           | V = 10 PV              | V = 6 PV      | V = 8 PV      | V = 10 PV     |
| Exp. 2 | 1400 ± 20 mD | Hematite suspension | <u>Deionized water</u> |               |               |               |
|        |              |                     | pH 7                   | pH 9          | pH 11         | pH 12         |
|        |              | Q = 25 mL/min       | Q = 10 mL/min          | Q = 10 mL/min | Q = 10 mL/min | Q = 10 mL/min |
|        |              | V = 30 PV           | V = 8 PV               | V = 6 PV      | V = 10 PV     | V = 20 PV     |

Table 3 – Permeability of the core sample before and after Exp. 1

|           | Permeability before,<br>mD ( $\mu\text{m}^2 \cdot 10^3$ ) | Permeability after, mD<br>mD ( $\mu\text{m}^2 \cdot 10^3$ ) | <u>Permeability impairment</u> |
|-----------|---|---|--------------------------------|
| Total     | 1770  | 590   | 67 %                           |
| Section 1 | 1760  | 270   | 85 %                           |
| Section 2 | 1780  | 1010  | 43 %                           |
| Section 3 | 1760  | 950   | 46 %                           |

Table 4 – Permeability of the core sample before and after Exp. 2

|           | Permeability before,<br>mD ( $\mu\text{m}^2 \cdot 10^3$ ) | Permeability after,<br>mD ( $\mu\text{m}^2 \cdot 10^3$ ) | <u>Permeability impairment</u> |
|-----------|---|--|--------------------------------|
| Total     | 1460  | 240  | 84 %                           |
| Section 1 | 1470  | 90   | 94 %                           |
| Section 2 | 1460  | 500  | 66 %                           |
| Section 3 | 1450  | 430  | 70 %                           |